Tunnelling under squeezing rock conditions

Giovanni Barla ([1])

([1]) Department of Structural and Geotechnical Engineering, Politecnico di Torino

Abstract: This lecture deals with tunnelling under squeezing rock conditions. Following an outline of the main factors influencing squeezing, the definition of this type of behaviour, as proposed by ISRM (International Society for Rock Mechanics) in 1995, is given. An overview of the methods used for identification and quantification of squeezing is presented, along with the empirical and semi-empirical approaches presently available in order to anticipate the potential of squeezing tunnel problems. A brief historical retrospective is reported on the excavation and support methods used in Italy in order to cope with squeezing conditions at the end of 1800, when the first railway tunnels were excavated. Based on the experiences made and lessons learned in recent years through important tunnelling works in Europe, an attempt is made to trace the state of the art in modern construction methods, when dealing with squeezing conditions by either conventional or mechanised excavation. The closed-form solutions available for the analysis of the rock mass response during tunnel excavation are described in terms of the ground characteristic line and with reference to some elasto-plastic or elasto-visco-plastic stress-strain models for the rock mass. Also described are the equations for the support characteristic lines. Then, the use of numerical methods for the simulation of different models of behaviour and for design analysis of complex excavation and support systems is considered, also including three-dimensional conditions near the advancing tunnel face. Finally, a brief discussion on monitoring methods is given, in conjunction with a short description of a case study.

1. Introduction

Squeezing stands for large time-dependent convergence during tunnel excavation. It takes place when a particular combination of induced stresses and material properties pushes some zones around the tunnel beyond the limiting shear stress at which creep starts. Deformation may terminate during construction or continue over a long period of time (Barla, 1995) ([1]).

The magnitude of tunnel convergence, the rate of deformation and the extent of the yielding zone around the tunnel depend on the geological and geotechnical conditions, the in-situ state of stress relative to rock mass strength, the groundwater flow and pore pressure, and the rock mass properties. Squeezing is therefore synonymous with yielding and time-dependence; it is closely related to the excavation and support techniques which are adopted. If the support installation is delayed, the rock mass moves into the tunnel and a stress redistribution takes place around it. On the contrary, if deformation is restrained, squeezing will lead to long-term load build-up of rock support.

The squeezing behaviour during tunnel excavation has intrigued experts for years, resulting in great difficulties for completing underground works, with major delays in construction schedules and cost overruns. There are numerous cases of particular interest in Europe where squeezing phenomena have occurred, providing some insights into the ground response during excavation. These include: the Cristina tunnel in Italy, the Gotthard tunnel in Switzerland, the Simplon tunnel crossing the Italian-Swiss border, just to mention some railway tunnels excavated between 1860 and 1910.

The technical reports and papers available describing such case-histories are likely to emphasize the phenomenological aspects and behaviour with reference to ground response during excavation, mostly in relation to the excavation methods and support sequence adopted. Even today, with significant steps forward in Geotechnical Engineering, the fundamental mechanisms of squeezing are not fully understood, as pointed out in a recent paper by Kovari (1998), also see Barla G. (2000). However, the close study of a number of more recent cases where detailed data are available (e.g. the Frejus Tunnel, Panet 1996; a number of tunnels in Japan, Aydan et al., 1993; the San Donato tunnel, Barla et al., 1986; etc.), let one derive the following remarks:

- The squeezing behaviour is associated with poor rock mass deformability and strength properties; based upon previous experience, there are a number

([1]) Definitions of squeezing as published by the International Society for Rock Mechanics (ISRM) Commission on Squeezing Rock in Tunnels are reported in Appendix 1, where also given is a summary of information regarding similar definitions available in the Rock Mechanics literature.

of rock complexes where squeezing will occur, if the loading conditions needed for the onset of squeezing are present: gneiss, micaschists and calcschists (typical of contact and tectonized zones and faults), claystones, clay-shales, marly-clays, etc.

- The squeezing behaviour implies that yielding will occur around the tunnel; the onset of a yielding zone in the tunnel surround determines a significant increase in tunnel convergences and face displacements (extrusion); these are generally large, increase in time and form the most significant aspects of the squeezing behaviour.
- The orientation of discontinuities, such as bedding planes and schistosities, plays a very important role in the onset and development of large deformations around tunnels, and therefore also on the squeezing behaviour. In general, if the main discontinuities strike parallel to the tunnel axis, the deformation will be enhanced significantly, as observed in terms of convergences during face advance.
- The pore pressure distribution and the piezometric head are shown to influence the rock mass stress-strain behaviour. Drainage measures causing a reduction in piezometric head and control both in the tunnel surround and ahead of the tunnel face help inhibiting development of ground deformations.
- The construction techniques for excavation and support (i.e. the excavation sequences and the number of excavation stages which are adopted, including the stabilization measures which are undertaken) may influence the overall stability conditions of the excavation. In general, the ability to provide an early confinement on the tunnel periphery and in near vicinity to the face, is accepted to be the most important factor in controlling ground deformations.

The large deformations associated with squeezing may also occur in rocks susceptible to swelling. Although the causes resulting in either a behaviour or the other one are different, it is often difficult to distinguish between squeezing and swelling, as the two phenomena may occur at the same time and induce similar effects. For example, in overconsolidated clays, the rapid stress-relief due to the tunnel excavation causes an increase in deviatoric stresses with simultaneous onset of negative pore pressure. In undrained conditions, the ground stresses may be such as not to cause squeezing. However, due to the negative pore pressure, swelling may occur with a more sudden onset of deformations under constant loading. Therefore, if swelling is restrained by means of early invert installation, a stress increase may take place with probable onset of squeezing.

2. Identification and quantification of squeezing conditions

In the landmark paper on tunnelling by Karl Terzaghi (1946), "*Rock defects and loads on tunnel supports*", the following definition of squeezing rock is given: "*Squeezing rock is merely rock which contains a considerable amount of clay. The clay may have been present originally, as in some shales, or it may be an alteration product. The rock may be mechanically intact, jointed, or crushed. The clay fraction of the rock may be dominated by the inoffensive members of the Kaolinite group or it may have the vicious properties of the Montmorillonites. Therefore the properties of squeezing rock may vary within as wide a range as those of clay*". When proceeding a little further, with the purpose to "*inform the tunnel builder on the steps required to get a conception of the pressure and working conditions which have to be anticipated in the construction of a proposed tunnel at a given site*", Terzaghi gives a behavioural description of squeezing rock as follows: *'Squeezing rock slowly advances into the tunnel without perceptible volume increase. Prerequisite of squeeze is a high percentage of microscopic and sub-microscopic particles of micaceous minerals or of clay minerals with a low swelling capacity".*

Based on the above description, which is meant to "identify" a rock condition with squeezing behaviour at the design stage and during excavation, a range of values for the "rock load" (not applicable for tunnels wider than 9 m) is given by Terzaghi for rock mass classes 7 and 8 which relate to squeezing:

"Rock Condition"	"Rock Load H_p in m of rock on roof of support for m of tunnel length"
Class 7: squeezing rock, moderate depth	(1.10 to 2.10) $(B+H_t)$
Class 8: squeezing rock, great depth	(2.10 to 4.50) $(B+H_t)$

when B (m) and H_t (m) are the width and height of the tunnel at depth more than 1.5 $(B+H_t)$.

The above is perhaps the first attempt in rock mechanics and tunnelling to "quantify" the squeezing potential of rocks in terms of loading of the initial support. Following Terzaghi, a number of approaches have been proposed by various authors, based on practical experience and documented case histories, to identify squeezing rock conditions and potential tunnel squeezing problems. In cases, as discussed below, the attempt has also been made to give an indication of the types of solutions that can be considered in overcoming these problems.

2.1 Empirical approaches

The empirical approaches are essentially based on classification schemes. Two of these approaches are mentioned below, in order to illustrate the uncertainty that still exists on the subject, notwithstanding its importance in tunnelling practice.

- **Singh et al. (1992) approach**

Based on 39 case histories, by collecting data on rock mass quality Q (Barton et al. 1974) and overburden H, Singh et al. (1992) plotted a clear cut demarcation line to differentiate squeezing cases from non-squeezing cases as shown in Figure 1. The equation of this line is

$$H = 350\ Q^{1/3}\ \text{[m]} \tag{1}$$

with the rock mass uniaxial compressive strength s_{cm} estimated as

$$s_{cm} = 0.7\ g\ Q^{1/3}\ \text{[MPa]} \tag{2}$$

with:
g = rock mass unit weight.

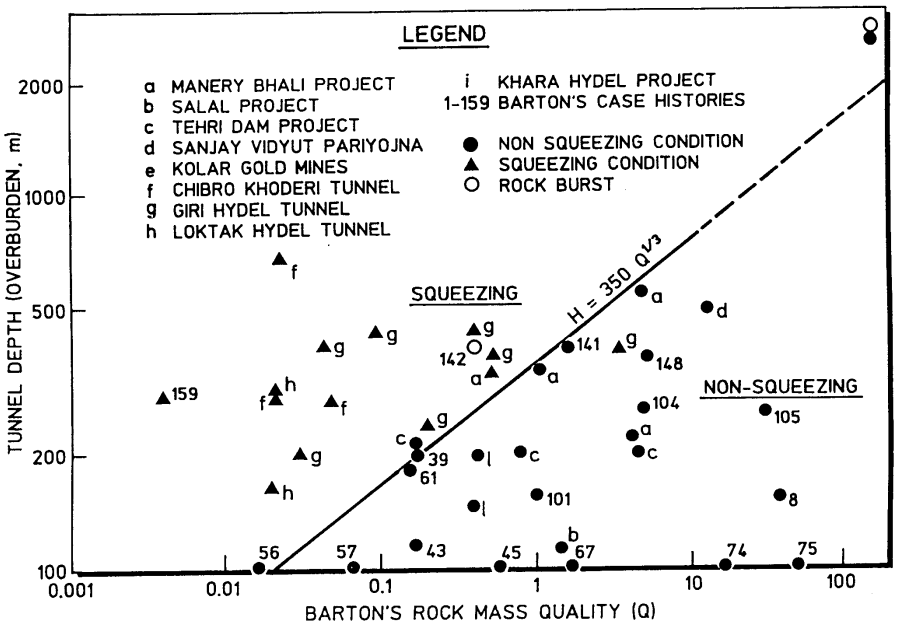

Figure 1: Singh et al. (1992) approach for predicting squeezing conditions

The data points lying above the line represent squeezing conditions, whereas those below this line represent non squeezing conditions. This can be summarized as follows:

for squeezing conditions

$$H >> 350\ Q^{1/3}\ [\text{m}] \tag{3}$$

for non squeezing conditions

$$H << 350\ Q^{1/3}\ [\text{m}] \tag{4}$$

- **Goel et al. (1995) approach**

A simple empirical approach developed by Goel et al. (1995) is based on the rock mass number *N*, defined as stress-free *Q* as follows:

$$N = (Q)_{SRF\,=\,1} \tag{5}$$

which is used to avoid the problems and uncertainties in obtaining the correct rating of parameter *SRF* in Barton et al. (1974) *Q*.

Considering the tunnel depth H, the tunnel span or diameter *B*, and the rock mass number *N* from 99 tunnel sections, Goel et al. (1995) have plotted the available data on a log-log diagram (Figure 2) between *N* and $H \cdot B^{0.1}$. As shown in the same Figure 2, a line demarcates the squeezing and non squeezing cases. The equation of this line is

$$H = (275\ N^{\,0.33})\ B^{-1}\ [\text{m}] \tag{6}$$

The data points lying above the line represent squeezing conditions, whereas those below this line represent non-squeezing conditions. This can be summarized as follows:

for squeezing conditions

$$H >> (275\ N^{\,0.33})\ B^{-1}\ [\text{m}] \tag{7}$$

for non squeezing conditions

$$H << (275\ N^{\,0.33})\ B^{-1}\ [\text{m}] \tag{8}$$

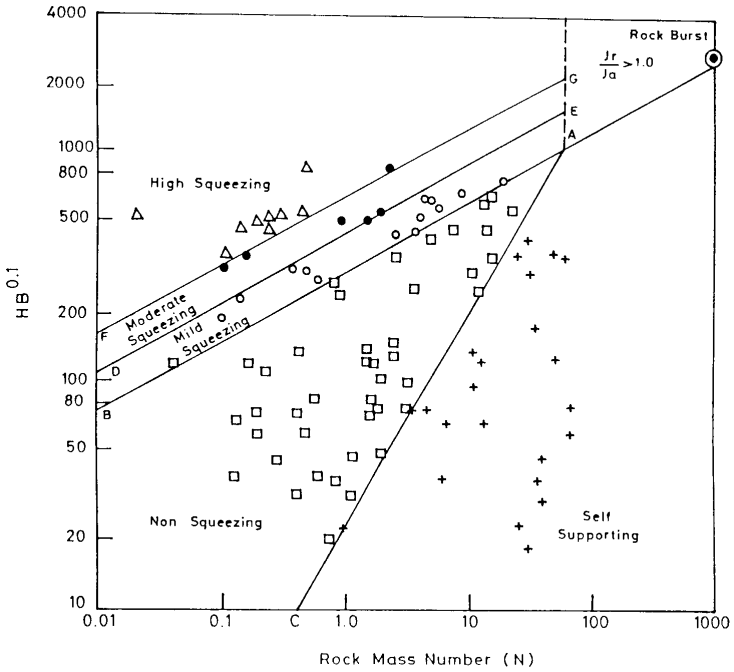

Figure 2: Goel et al. (1995), (2000) approach for predicting squeezing conditions

- **Degree of squeezing**

It may be added that for both the empirical approaches above, the degree of squeezing can be represented by tunnel convergence as follows (Singh and Goel, 1999):

(i) Mild squeezing convergence 1-3% tunnel diameter
(ii) Moderate squeezing convergence 3-5% tunnel diameter
(iii) High squeezing convergence >5% tunnel diameter.

2.2 Semi-empirical approaches

The empirical relationships above are intended to identify potential squeezing problems in tunnels, essentially in terms of the tunnel depth and rock mass quality (the Q or $(Q)_{SFR\,=\,1}$ index is used as shown). The semi-empirical approaches illustrated in the following are again giving indicators for predicting squeezing. However, they also provide some tools for estimating the expected deformation around the tunnel and/or the support pressure required, by using closed form analytical solutions for a circular tunnel in a hydrostatic stress field (see Chapter 4). The common starting point of all these methods for quantifying the squeezing potential of rock is the use of the "competency factor", which is

defined as the ratio of uniaxial compressive strength s_c/s_{cm} of rock/rock mass to overburden stress gH. Three of such methods are briefly discussed in the following.

- **Jethwa et al. (1984) approach**

As mentioned above the degree of squeezing is defined by Jethwa et al. (1984) on the basis of the following (see Table 1 below):

$$N_c = \frac{\sigma_{cm}}{p_0} = \frac{\sigma_{cm}}{\gamma H} \tag{9}$$

where:
σ_{cm} = rock mass uniaxial compressive strength;
p_0 = in situ stress;
γ = rock mass unit weight;
H = tunnel depth below surface.

Table 1: Classification of squeezing behaviour according to Jethwa et al. (1984)

$\frac{\sigma_{cm}}{p_0}$	type of behaviour
<0.4	highly squeezing
0.4-0.8	moderately squeezing
0.8-2.0	mildly squeezing
>2.0	non squeezing

By using an analytical closed form solution for a circular tunnel under a hydrostatic stress field and data from in situ monitoring, an expression for the ultimate rock pressure p_u on the tunnel lining is given as follows:

$$\frac{p_u}{p_0} = D \cdot M_f \left(1 - \sin \phi_p\right) \left(1 - \frac{\sigma_{cm}}{2 p_0}\right) \tag{10}$$

where:

$$D = \frac{\left(R_c / R\right)^a - \left(R / R_c\right)^2}{1 - \left(a / R_c\right)^2} \tag{11}$$

$$M_f = \left(R / R_{p_l}\right)^{\alpha} \tag{12}$$

$$\sigma_{cm} = \frac{2c_p \cos\varphi_p}{1-\sin\varphi_p}, \alpha = \frac{2\sin\varphi_r}{1-\sin\varphi_r} \tag{13}$$

for: R = tunnel radius; R_c = radius of compacting zone in contact with the lining; R_{pl} = radius of plastic zone; c_p, c_r and φ_p, φ_r = rock mass cohesion and friction values (peak and residual values respectively).

As shown in Figure 3, a plot of the p_u / p_0 ratio is given versus φ_p, for different values of $\sigma_{cm} / 2p_0$ and a set of residual friction angles φ_r, always for a residual cohesion c_r equal to zero ([2]).

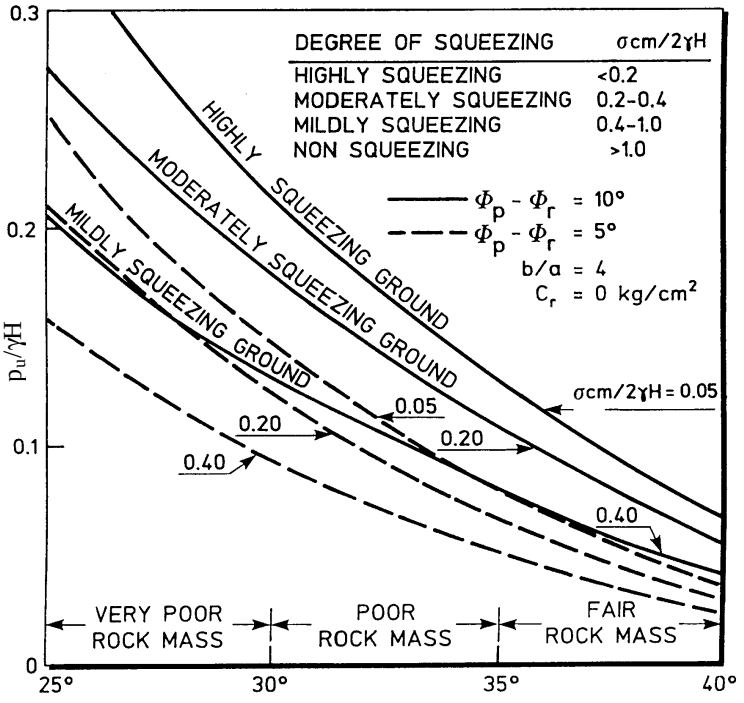

Figure 3: Jethwa et al. (1984) approach for predicting squeezing conditions

([2]) As described in the following, the assumption introduced is that the rock mass behaves according to an elastic-plastic ideally brittle model with a Mohr-Coulomb strength criterion ($c_p \neq c_r$; $\varphi_p \neq \varphi_r$).

- **Aydan et al. (1993) approach**

Aydan et al. (1993), based on the experience with tunnels in Japan, proposed to relate the strength of the intact rock s_{ci} to the overburden pressure gH by the same relation as (9), by implying that the uniaxial compressive strength of the intact rock s_{ci} and of the rock mass s_{cm} are the same. As shown in Figure 4, which gives a plot of data of surveyed tunnels in squeezing rocks in Japan, squeezing conditions will occur if the ratio s_c / gH is less than 2.0.

The fundamental concept of the method is based on the analogy between the stress-strain response of rock in laboratory testing and tangential stress-strain response around tunnels. As illustrated in Figure 5, five distinct states of the specimen during loading are experienced, at low confining stress s_3 (i.e. $s_3 \leq 0.1 s_{ci}$). The following relations are defined which give the normalized strain levels h_p , h_s and h_f :

$$h_p = \frac{e_p}{e_e} = 2 s_{ci}^{-0.17}, h_s = \frac{e_s}{e_e} = 3 s_{ci}^{-0.25}, h_f = \frac{e_f}{e_e} = 5 s_{ci}^{-0.32} \qquad (14)$$

where e_p, e_s and ε_f are the strain values shown in Figure 5, as e_e is the elastic strain limit.

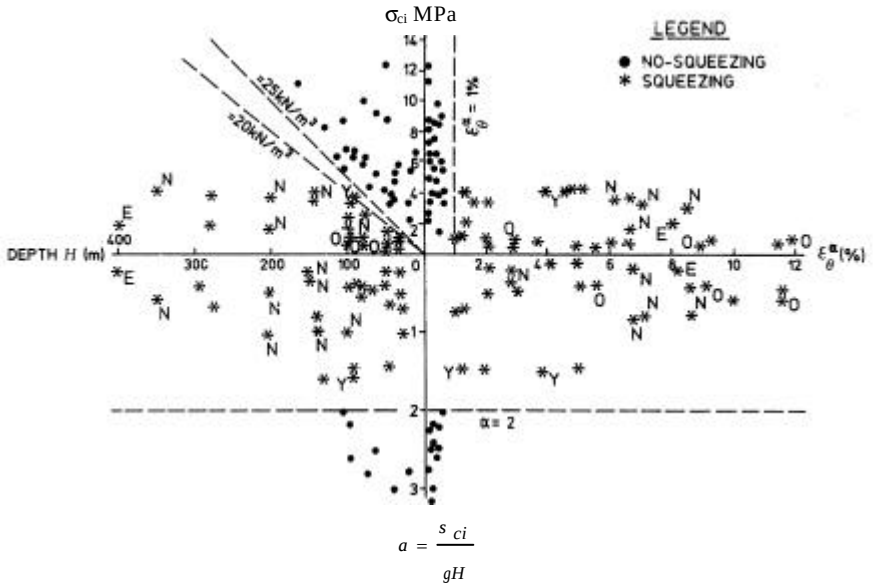

Figure 4: Aydan et al. (1993) approach for predicting squeezing conditions

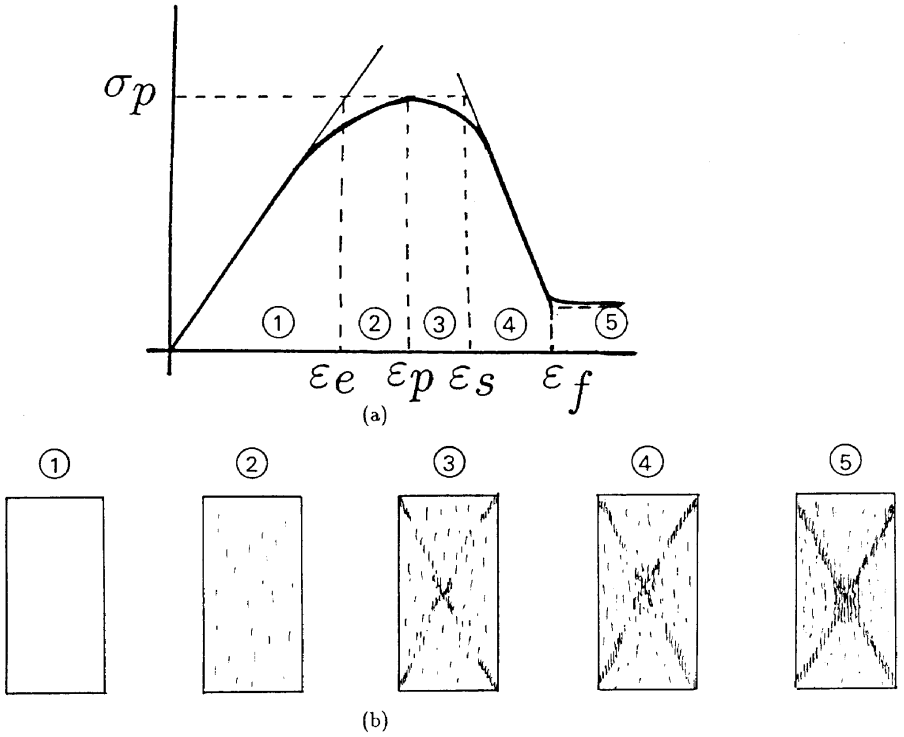

Figure 5: Idealised stress-strain curve and associated states for squeezing rocks (Aydan et al., 1993)

Based on a closed form analytical solution, which has been developed for computing the strain level e_q^a around a circular tunnel in a hydrostatic stress field, the five different degree of squeezing are defined as shown in Table 2, where also given are some comments on the expected tunnel behaviour.

Table 2: Classification of squeezing behaviour according to Aydan et al. (1993)

class no.	squeezing degree	symbol	theoretical expression	comments on tunnel behaviour
1	non-squeezing	NS	$e_q^a / e_q^e \leq 1$	the rock behaves elastically and the tunnel will be stable as the face effect ceases
2	light-squeezing	LS	$1 < e_q^a / e_q^e \leq \eta_p$	the rock exhibits a strain-hardening behaviour. As a result, the tunnel will be stable and the displacement will converge as the face effect ceases
3	fair-squeezing	FS	$\eta_p < e_q^a / e_q^e \leq \eta_s$	the rock exhibits a strain-softening behaviour and the displacement will be larger. However, it will converge as the face effect ceases
4	heavy-squeezing	HS	$\eta_s < e_q^a / e_q^e \leq \eta_f$	the rock exhibits a strain-softening at much higher rate. Subsequently, displacement will be larger and it will not tend to converge as the face effect ceases
5	very heavy-squeezing	VHS	$\eta_f < e_q^a / e_q^e$	the rock flows, which will result in the collapse of the medium and the displacement will be very large and it will be necessary to re-excavate the opening and install heavy supports

Note: for η_p, η_s and η_f see equation (14); $\varepsilon_q^{\breve{}}$ is the tangential strain around a circular tunnel in a hydrostatic stress field (Aydan et al., 1993), whereas $\varepsilon_q^{\breve{}}$ is the elastic strain limit for the rock mass.

- **Hoek and Marinos (2000) approach**

As the previous authors, Hoek (1998) used the ratio of the rock mass uniaxial compressive strength s_{cm} to the in situ stress p_0 as an indicator of potential tunnel squeezing problems. In particular, Hoek and Marinos (2000) showed that a plot of tunnel strain e_t (defined as the percentage ratio of radial tunnel wall displacement to tunnel radius, i.e. the same strain as e_q^a given by Aydan et al., 1993) against the ratio s_{cm} / p_0 can be used effectively to assess tunnelling problems under squeezing conditions.

Hoek (2000), in his recent 2000 Terzaghi lecture on "*Big tunnels in bad rock*", by means of axi-symmetric finite element analyses and a range of different rock masses, in situ stresses and support pressures p_i gave the following approximate relationship for the tunnel strain ε_t

$$e_t(\%) = 0.15(1 - p_i / p_o)\frac{s_{cm}}{p_o}^{-(3p_i / p_o + 1)/(3.8p_i / p_o + 0.54)} \qquad (15)$$

Similarly, by recognizing the importance of controlling the behaviour of the advancing tunnel face in squeezing rock conditions, Hoek (2000) gave the following approximate relationship for the strain of the face ε_f (defined as the percentage ratio of axial face displacement to tunnel radius)

$$e_f(\%) = 0.1(1 - p_i / p_o)\frac{s_{cm}}{p_o}^{-(3p_i / p_o + 1)/(3.8p_i / p_o + 0.54)} \qquad (16)$$

In order to get a good understanding of the trend of deformational behaviour around the tunnel as suggested by the equations (15) and (16), Figure 6 plots ε_t and ε_f for a range of s_{cm} / p_0 values and internal support pressure p_i.

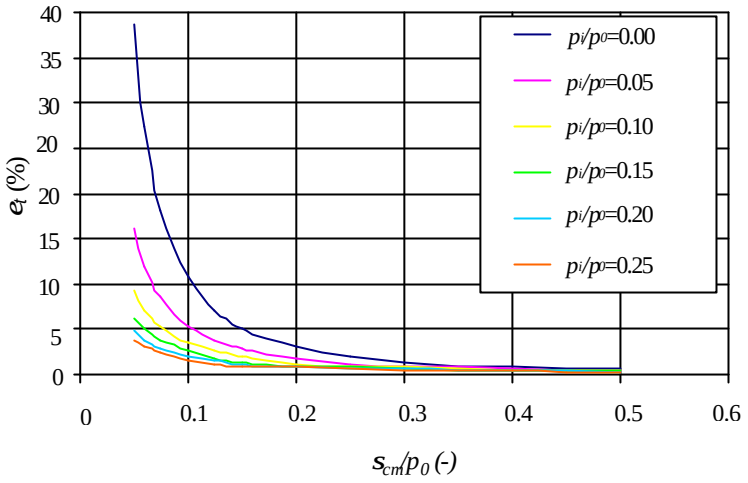

(a)

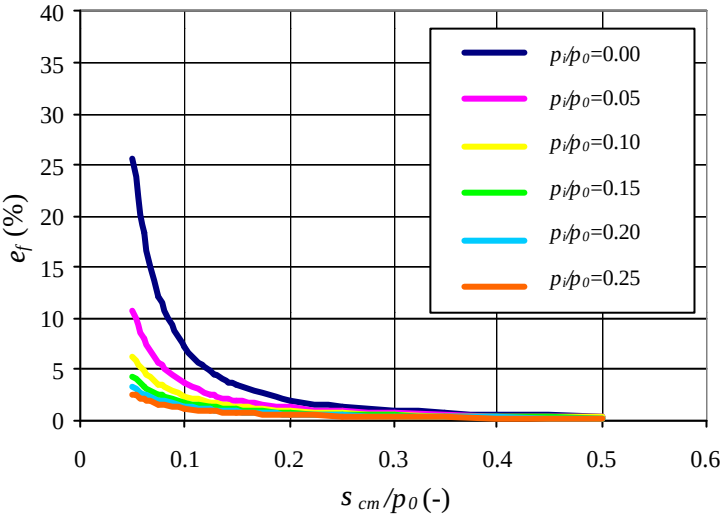

(b)

Figure 6: (a) tunnel strain e_t; (b) face strain ε_f for a range of s_{cm} / p_0 values and internal support pressure p_i

On the basis of the above and consideration of case histories for a number of tunnels in Venezuela, Taiwan and India ([3]), Hoek (2000) gave the curve of Figure 7 to be used as a first estimate of tunnel squeezing problems. In order to compare with the previously reported classes of squeezing conditions as given by Aydan et al. (1993), Table 3 below gives the range of tunnel strains expected in the two cases.

Table 3: Classification of squeezing behaviour according to Hoek (2000) compared with Aydan et al. (1993) classification

	Aydan et al. (1993) ([4])		Hoek (2000)	
class no.	squeezing level	tunnel strain (%)	squeezing level	tunnel strain (%)
1	no-squeezing	$e_q^a \leq 1$	few support problems	$e_t \leq 1$
2	light-squeezing	$1 < e_q^a \leq 2.0$	minor squeezing	$1 < e_t \leq 2.5$
3	fair-squeezing	$2.0 < e_q^a \leq 3.0$	severe squeezing	$2.5 < e_t \leq 5.0$
4	heavy-squeezing	$3.0 < e_q^a \leq 5.0$	very severe squeezing	$5.0 < e_t \leq 10.0$
5	very heavy-squeezing	$e_q^a \leq 5.0$	extreme squeezing	$e_t > 10.0$

([3]) The tunnel cases considered include 16 tunnels in graphitic phyllites, sandstone, shale, slates, fractured quartzite, sheared metabasic rocks and fault zones. The tunnel span ranged from 4.2 m to 16 m, with two cases equal to 2.5 and 3 m respectively. The overburden is from 110 m to 480 m, with two cases up to 600 m and 800 m respectively.

([4]) The intact rock strength s_{ci} is assumed to be 1 MPa.

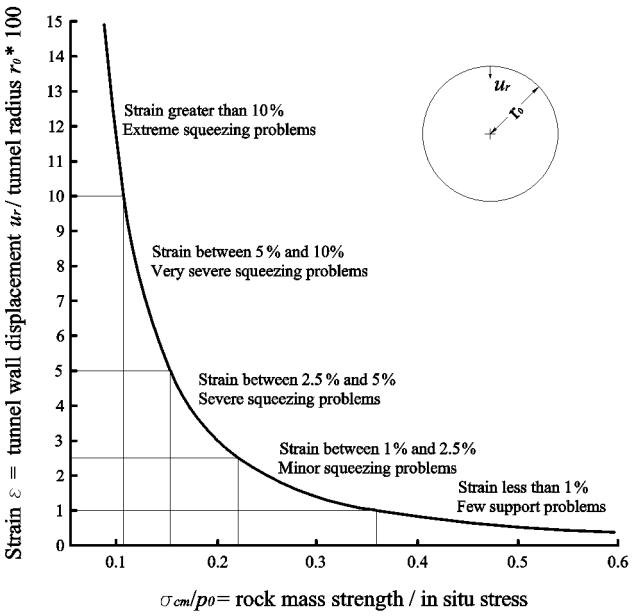

Figure 7: Classification of squeezing behaviour (Hoek, 2000)

- **Uncertainties on rock mass strength**

The identification and quantification of squeezing behaviour based on semi-empirical approaches make it essential to know the rock mass uniaxial compressive strength s_{cm}. For example, if the ratio s_{cm} / p_0 is known, according to Hoek (2000) one can estimate, for a wide range of conditions, the strain of the tunnel e_t and of the face e_f by using equations (15) and (16).
It is clear that the approach, although useful for estimating potential tunnelling problems due to squeezing conditions, is not a substitute for more sophisticated methods of analysis. However, even with this in mind, the difficulty remains that the selection of reliable rock mass properties is a difficult task. A possible way to estimate s_{cm}, which has been recently proposed by Hoek and Marinos (2000), is to use the following equation:

$$s_{cm} = \left(0.0034 m_i^{0.8}\right) \; s_{ci} \left[1.029 + 0.025 e^{(-0.1 m_i)}\right]^{GSI} \qquad (17)$$

where:

s_{ci} = uniaxial compressive strength of the intact rock;
m_i = Hoek-Brown constant, defined by the frictional characteristics of the component materials in the rock, is determined by triaxial testing on

core samples or estimated from a qualitative description of the rock material as described by Hoek and Brown (1997);

GSI = Geological Strength Index, that relates the properties of the intact rock to the overall rock mass, was introduced by Hoek et al. (1995), Hoek and Brown (1997), and extended by Hoek et al. (1998).

In most cases, when dealing with rock masses which exhibit a squeezing behaviour, the evaluation of s_{ci} and m_i may become a hard task as it is extremely difficult, to obtain samples of intact rock for testing in the laboratory. The evaluation of the *GSI* index is based on visual examination of the rock mass exposed in tunnel faces, surface excavation and in borehole cores. However, this is difficult and highly subjective, when referred to the rock conditions typical of tunnels which undergo severe squeezing problems.

3. Excavation and support methods

The excavation and support methods used when tunnelling under squeezing rock conditions have evolved slowly through experience gained in different rock masses, a series of successes and failures, in different parts of the world, although most of all in Europe and Japan. Even when accounting for the many lessons learned and reported in the rock mechanics and tunnelling literature, it is difficult to draw conclusions on the most reliable methods to be used when dealing with such conditions. Our attempt is to report here some of the general trends in excavation and support methods in squeezing rock conditions, following a brief historical retrospective in the early days of "modern" tunnelling.

3.1 Brief historical retrospective

Excavation and support methods in the early days of "modern" tunnelling consisted in using pilot drift driving in either the crown or the invert of the future tunnel cross section. This drift was supported primarily by timber and enlarged to the full cross section of the tunnel in multiple stages, always using a support with timber. When the tunnel was excavated to the full size, the final masonry lining (cut stones or lime-sand-cement bricks) was installed and the timber support removed.

To put in writing a curious record of this period of tunnelling, it is of interest to reproduce in Figures 8 and 9 two wooden models of these methods of tunnel driving taken from the Politecnico di Torino Museum. Here, a fascinating collection of models is kept, as used between 1860 and 1880 in the form of a teaching aid in the course of Strength of Materials, in the former School of Engineering Applications in Torino. Figure 8 shows a model of the "Belgian exca-

vation sequence or method", where the tunnel support is installed in the upper cross section, before benching down. Figure 9 illustrates instead the so-called "Italian method", which was applied following a proposal by Luigi Protche in the Cristina tunnel (along the "*Traversata dell'Appennino nella Linea Foggia-Napoli*", Apennines Railway Crossing, between Foggia and Naples), under extremely severe squeezing and swelling conditions (Lanino, 1875).

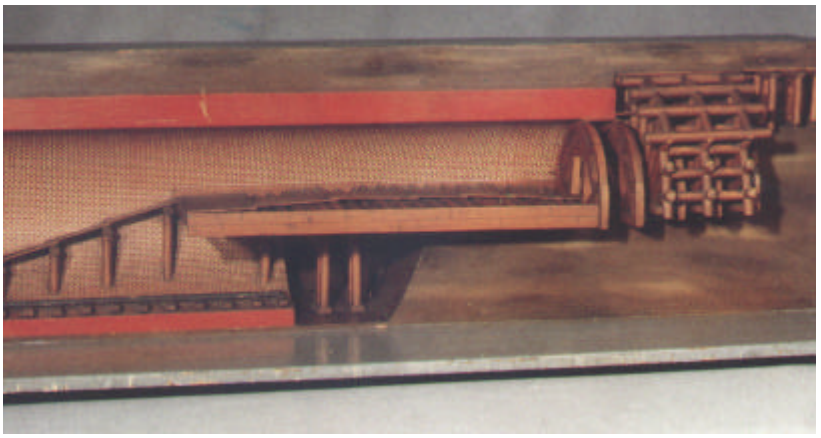

Figure 8: Photograph of a wooden model representing the Belgian excavation sequence in tunnelling (Courtesy of the Politecnico di Torino Museum)

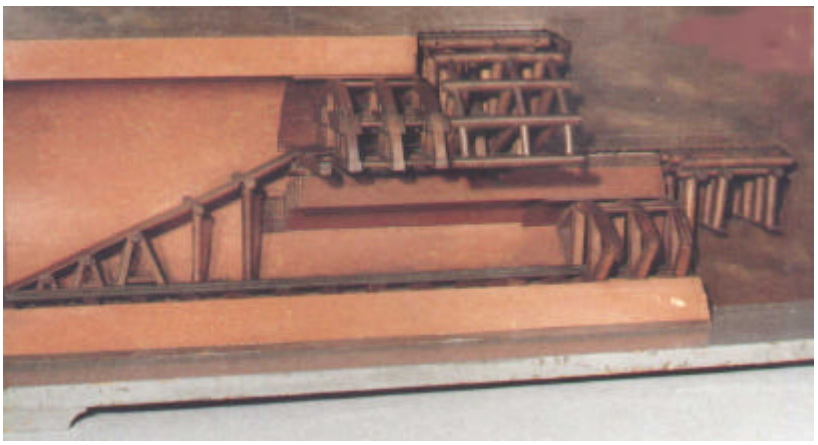

Figure 9: Photograph of a wooden model representing the Italian excavation sequence in tunnelling (Courtesy of the Politecnico di Torino Museum)

The latter method is of great interest with reference to excavation in squeezing rocks, so that some attention will be paid to it in order to better understand the steps made in the last 140 years by reaching the present methods of excavating and supporting a tunnel in such conditions, which will be discussed in the fol-

lowing. As shown in the illustration of Figure 10, a small size drift is advanced at the base of the tunnel as a brick masonry invert is installed immediately behind by closing up the lower cross section, before starting the excavation of the top heading.

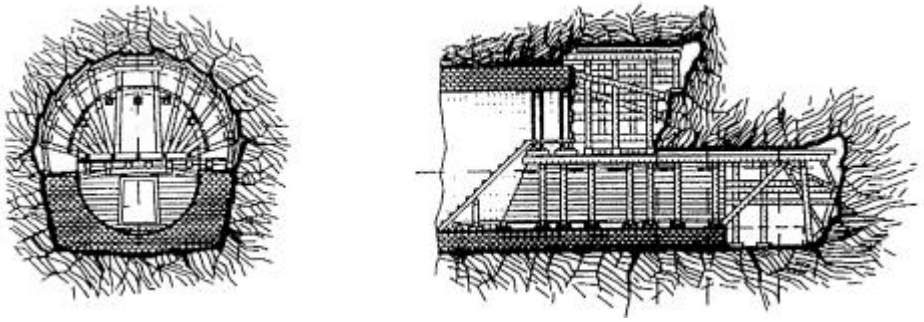

Figure 10: A sketch of the Italian method of excavating and supporting a tunnel in squeezing rock conditions applied in the Cristina tunnel (Lanino, 1875)

It is of interest to report here the motivations given by the miners of the time to explain why the excavation method by starting the tunnel in the lower cross section was successful (under extremely severe squeezing conditions associated with swelling, as experienced in the scaly clay complex of the Cristina tunnel), where the top heading and benching down method was not (Lanino, 1875, see Figure 10):

- "the excavation takes place in very short steps, as the full cross section of the tunnel is closed completely before moving to the next ring": a 3 m length, equivalent to a ring, was excavated and completed with the final brick masonry lining in 16 days;
- "the tunnel invert is installed as the first structural component in the section" and, "with the lower cross section filled up, the lining at the sidewalls is kept from converging significantly, and a strong action is set in place to keep the tunnel face stable".

A number of important factors appeared to be well known and considered to be essential, more than 140 years ago, for controlling the stability of the face and of the tunnel in squeezing conditions (Lanino, 1875):

- with the top heading and benching down method the upper cross section of the tunnel cannot be maintained stable for a long time as progressive failure will occur at the sidewalls, the vault will sink and will be pushed horizontally into the cavity;

- with the excavation of the lower cross section, when this takes place at a significant distance from the working face zone, the stability conditions of the upper cross section become problematic and the completion of the final lining nearly impossible.

By completing the lower cross section first, a foundation for the subsequent placement of the vault in the heading was made available and, at the same time, a significant resistance was being provided at the sidewalls and invert. By keeping the distance between the two working faces (the lower and upper one) to a minimum and closing "quickly" the full cross section with the masonry lining, "not too far from the same working faces", the tunnel could be excavated, at a very limited rate of advance even for the time under consideration, more than 140 years ago (6 m of completed tunnel in a month!).

3.2 Conventional methods

If attention is paid to current trends for construction of tunnels with spans greater than 10 m (100 m^2 size or more) under squeezing rock conditions, depending on the measures taken to prevent or bring under control the large deformations that would take place during excavation, the following conventional construction methods are being applied (Figure 11):

- side drift method
- top heading and benching down excavation
- full face excavation.

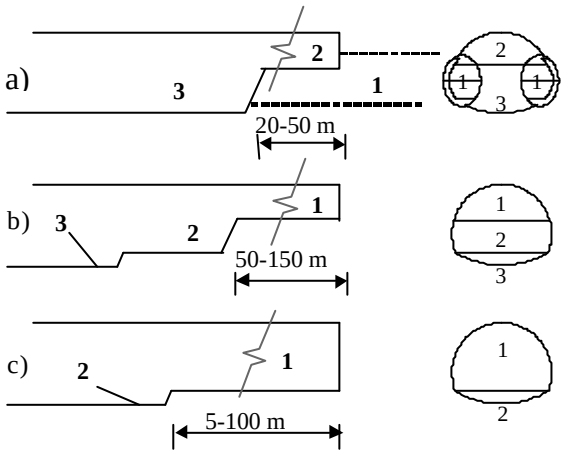

Figure 11: Construction methods in squeezing rock conditions (Kovari, 1998):
a) side drift method
b) top heading and benching down excavation
c) full face excavation

- The **side drift method** of construction with advanced concrete sides has been widely applied in poor ground conditions as a mean to reduce the cross section open in one stage, thus reducing the potential of instability of the working face. This method is applied particularly if tunnels are at shallow depth. However, the reduced working conditions in the side drifts, associated with the many excavation/construction stages required in practice, result in very low rate of face advance.

Figures 12 and 13 show one possible side drift method for driving a tunnel through squeezing ground (typically, weathered clay-shales) as adopted in the Himmelberg North tunnel in Germany under a low cover of the order of 50-60 m. The tunnel has an excavated span of 15 m approximately. A 35-40 cm thick steel mesh reinforced shotcrete lining is being installed in line with 4-6 m long dowels. Drainage holes are driven ahead from the side drifts, and occasionally fiberglass dowels are installed for face support.

(a)

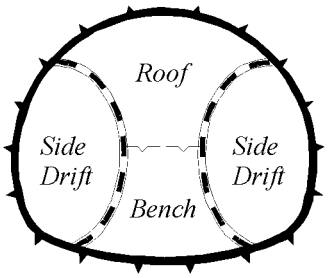

(b)

Figure 12: Typical side drift method as adopted during the excavation of the Himmelberg North Tunnel (photograph provided by Balbi, 1999)

Figure 13: Photographs showing the Himmelberg North Tunnel during excavation: (a) view of the full cross section with side drifts; (b) left side drift (photographs provided by Balbi, 1999)

- The **top heading and benching down excavation method** is usually applied today with a heading height of 5.0 m or more, so as to permit a high degree of mechanization for implementation of stabilization measures, if required, and support placement. The benching down is carried out at a later stage than the top heading at a distance from the face which is dependent upon the ground response during excavation. It is not unusual, in very poor ground conditions, to install a shotcrete invert as a footing of the top heading, in order to prevent excessive deformations from developing and to control floor heave.

By paying attention to the top heading and benching down excavation method in practical cases, the need arises, in poor to very poor quality rock masses, to excavate the top heading under the protection of an umbrella of forepoles consisting of perforated pipes (either simply grouted along the pipe length or injected, Barla, 1989). A typical application for the S. Ambrogio tunnel along the Messina-Palermo Highway in Italy is shown in Figures 14 and 15.

A twin road tunnel with two lanes each has been excavated through a weak flysch with quartzitic-sandstone layers alternating with marl ($RMR \cong$ 30-40). Heavy steel sets and mesh reinforced shotcrete formed the primary support system used. Bench excavation took place at a short distance from the top heading working face (Figure 14), with the placement of the invert arch and ring closure as soon as possible (20÷25 m approximately), considering the need to install the forepole umbrella prior to any top heading advance.

Figure 14: Top heading and benching down excavation method, with placement of heavily steel reinforced invert arch at a short distance from the top heading working face. S. Ambrogio tunnel along the Palermo-Messina Highway in Italy

An additional provision which has been implemented, particularly in the case of excavation of tunnels at shallow depth and in very poor ground conditions, is to underpin the top heading by means of nearly vertical micropiles and to install nearly horizontal anchors on both sides (Figure 15). This avoids the top heading to be left without support when the bench is excavated and provides a very useful restraint against horizontal deformations that are likely to occur at the same time. Additionally, if needed, fiberglass dowels may be applied for face stabilization of the top heading.

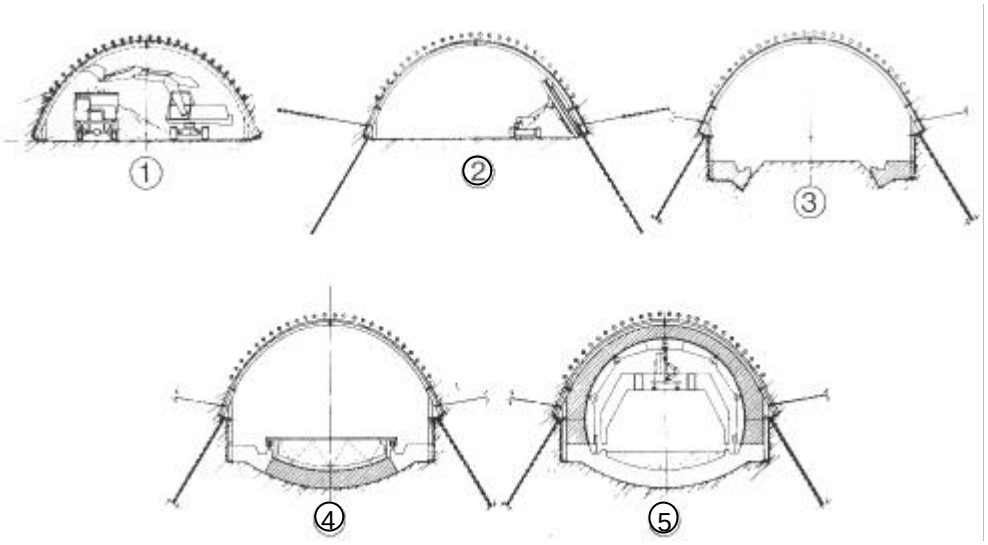

Figure 15: Top heading and benching down excavation method. 1-2: top heading excavation takes place under the protection of an umbrella of forepoles; 3-4: benching down is effected at short distance from the top heading working face; 5: final lining is installed for long term stability. S. Ambrogio tunnel along the Palermo-Messina Highway in Italy

- The **full face excavation method** in squeezing rock conditions is quite appealing and has been applied with success in many cases (Lunardi and Bindi, 2001). However, the method makes it mandatory to use a systematic reinforcement of the working face and of the ground ahead. It need be recognized, at the present stage, that although ground treatment techniques can be highly effective in controlling stability and ground movements, the methods for prediction and quantification of these beneficial effects at the design stage and during construction (even if performance monitoring of ground response ahead of the working face is implemented) are not yet well established and need further investigation.

The use of the full face excavation method is definitely being favoured at present by designers from Italy with respect to the top heading and benching down excavation method as described in Figure 15, which was the typical method adopted from 1985 to 1990 (Barla, 1989). The full face excavation method was introduced by Lunardi (1995) who was the first to suggest that "understanding and controlling the behaviour of the core ahead of the advancing tunnel face is the secret of successful tunnelling in squeezing rock conditions" (Hoek, 2000).

Figure 16 (a) and (b) shows a typical case of the full face excavation method adopted for the Morgex tunnel along the Aosta – Mont Blanc Highway, in Italy. The tunnel has an excavated span of 12.6 m and an 11.0 m span measured in-

side the final concrete lining. The excavation took place through very poor ground conditions (a "melange" of rock blocks in a clay, sand and gravel matrix) before reaching a fair to good calcschist rock mass, where the excavation was carried out by drill and blast.

A remarkable and successful application of the full face excavation method to the construction of a large size tunnel with 19 m maximum excavated span, in squeezing rock conditions associated with swelling behaviour, has been described by Lunardi et al. (2000) for the Tartaiguille tunnel, in France. The rock is a marly claystone with high montmorillonites content.

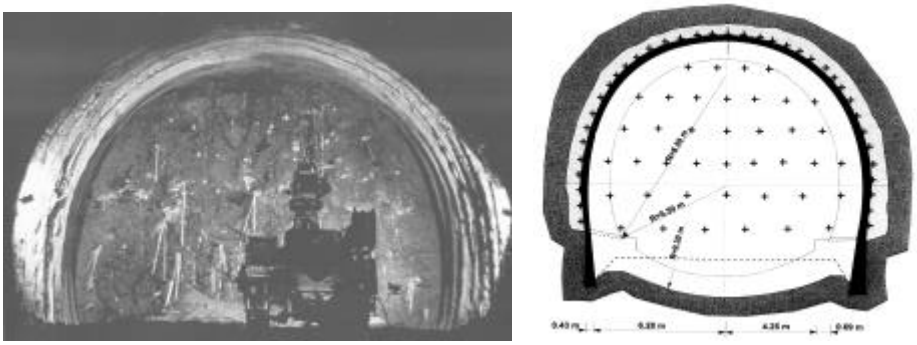

(a) (b)

Figure 16: Full face excavation method, with face stabilization by fully grouted fiberglass dowels, under the protection of forepole umbrella, Morgex tunnel along the Aosta-Mont Blanc Highway, in Italy: (a) photograph of the face supported by fully grouted fiberglass tubes; (b) schematic drawing of the full face excavation method with fiberglass tubes grouted in face

As illustrated in Figure 17, a total of 90 grouted fiberglass dowels (length 24 m) were used for face stabilization and reinforcement of the rock core ahead of the advancing face. Also to be noted in the procedure adopted for the Tartaiguille tunnel is that a reinforced concrete invert (Figure 17 (b)) used to be set in place at a short distance from the tunnel face (4 to 6 m), in order to keep the diametral convergence up to 5÷7 cm maximum. The primary lining consisted of a 30 cm thick fiber reinforced shotcrete and heavy steel sets spaced 1.33÷1.50 m.

It is quite obvious from the discussion above that with the full face excavation method a significant advantage is found in the large working space now available at the advancing face, so that a large equipment can be used effectively for installing support/stabilization measures at the tunnel perimeter and ahead of the face (as shown in Figure 18 below, which illustrates a large cross section tunnel – maximum excavated span 15 m (in the enlargement section) – being exca-

vated in Italy, near La Spezia. Here again the rock mass is very poor with argillite and sandstone alternating in a sequence of very thin layers exhibiting a squeezing behaviour ($RMR < 30$).

(a) (b)

Figure 17: Full face excavation method, Tartaiguille tunnel, in France: (a) photograph of the face; (b) photograph of reinforced concrete invert (Lunardi et al., 2000)

Figure 18: Full face excavation method, Marinasco tunnel near La Spezia, in Italy. Large equipment being used at the face

There is an additional point to raise in connection with the importance of the shape of the tunnel cross section when the excavation is undertaken in squeezing rock conditions. It is to be recognized that the horseshoe profile with straight side walls, as shown in Figures 14 and 15 is highly unfavourable with respect to the curved sidewalls used, for example, in the case of Figures 16 to 18.

• The construction method by one of the options shown in Figure 11 is closely dependent on the measures that are taken to stabilize the opening and the type of rock support which is used (steel sets, fully grouted bolts, mesh or fiber reinforced shotcrete, etc.). It is common for tunnelling in squeezing rock conditions to adopt either an **active** or a **passive** approach.

With the **active** approach, the so-called "heavy method" or "resistance principle", the objective is to prevent rock deformation to take place by means of a sufficiently strong support/stabilization/lining system. This course of action may however result in heavy loading of the support. One alternative way, always in terms of the "resistance principle", is the use of systematic pre-reinforcement and pre-treatment in advance of tunnelling, so as to inhibit the large deformations that would otherwise develop behind the working face.

With the **passive** approach, also called "light method" or "yielding principle", a number of constructions procedures are applied. They aim at accommodating the large deformations which develop in squeezing rock conditions. The support is allowed to yield in a controlled manner so that its capacity is only mobilized when a significant displacement has taken place. The following procedures are the most commonly used:

- **Over-excavation**: in order to obtain the required clearance profile following convergence, the tunnel is excavated to a magnitude which allows for support installation, including the permanent lining. In general, the decision on the amount of over-excavation is based on performance monitoring of tunnel behaviour in a previously excavated length, and engineering judgment.
- **Compression longitudinal slots in the shotcrete lining**: the shotcrete lining is divided into segments as shown in Figure 19, with the purpose to prevent load build up in the same lining leading to uncontrolled failure. This approach, first introduced in 1971 in the Tauern tunnel, has been successfully applied in the Arlberg and Karawanken tunnels, and more recently in the Inntal tunnel and in the Galgenberg tunnel, always with the objective to accommodate heavy squeezing rock conditions, Schubert (1996).

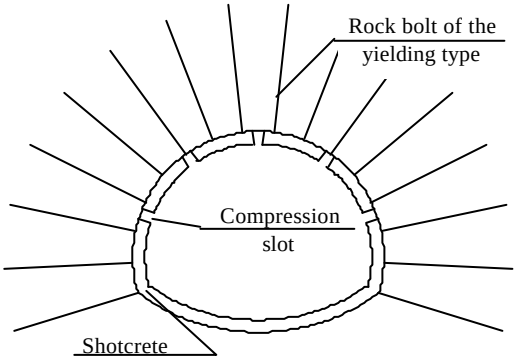

Figure 19: Cross section of a tunnel with compression slots applied in squeezing rock conditions (redrawn from Schubert W. and Schubert P., 1993)

The use of **longitudinal slots in the shotcrete lining** has been associated with the installation of TH (Toussaint – Heintzmann, also known as "Top Hat") profile steel sets nested and clamped to form a frictional sliding joint (Figure 20), and in cases with rock bolts which exhibit a yielding behaviour (Figure 21). A typical working sequence consists in installing these steel sets immediately behind the tunnel face, followed by placement of shotcrete and rock bolts, however leaving a slot for each sliding joint. This method became the conventional support method from 1975 to 1995 for controlling squeezing conditions in the Alps.

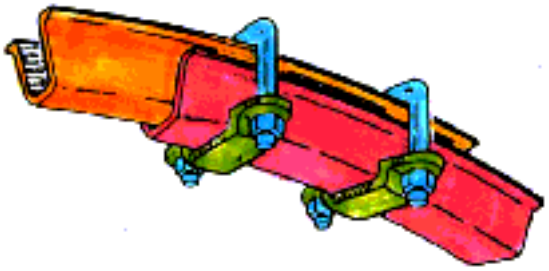

(a)

(b)

Figure 20: (a) assembly of a sliding joint in a TH section steel set; (b) cross section detail

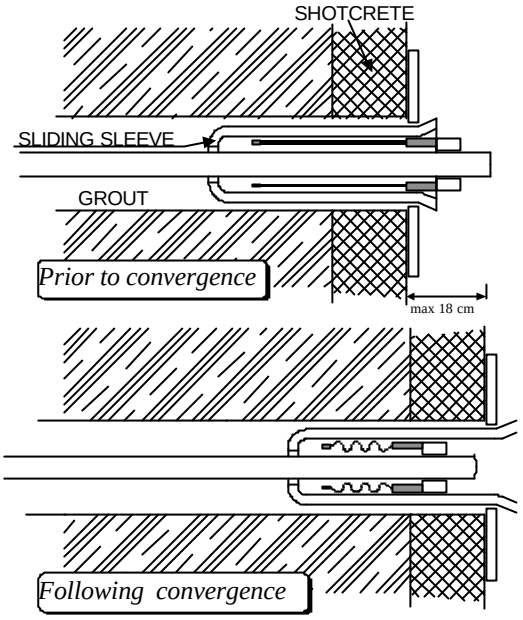

Figure 21: Typical yielding bolt as developed in connection with the excavation of the Karawanken Tunnel in squeezing rock conditions (redrawn from Schubert W. and Schubert P., 1993)

As reported by Schubert (1996), some concern on the practice to leave the slots open was raised, as this does not allow any thrust transmission between the single shotcrete segments unless these slots close before any deformation has stopped. If a rock mass shows a tendency for loosening, a certain thrust transmission between the segments is required, especially at an early stage, when the rock bolts are yet not fully active.

This led to the development of low cost “absorbing elements” in the form of steel pipes for installation in the slots between the shotcrete segments, while maintaining a sufficient ductility to the shotcrete lining in order to prevent shearing. This system, which was used in the Galgenberg tunnel (Figure 22) in combination with regroutable rock bolts, permitted a considerable reduction of tunnel convergence and an increase in safety, without requiring any reshaping of the tunnel cross-section.

One of the disadvantages of the steel pipes was found in the extreme oscillation of the load-displacement curve, which is caused by the strong decrease in load bearing capacity after the resistance against buckling is exceeded. Another problem reported is the possibility of asymmetric buckling and non symmetric folding of the single pipes.

Figure 22: "Galgenberg Tunnel" (Austria), yielding-steel-elements installed in deformation slots of the shotcrete lining (Moritz, 1999)

The most recent developments regarding the use of compression slots are described in a Ph.D. thesis by Dr. Moritz of the University of Graz (Austria), who modified the "absorbing elements" by introducing an advanced system, called Lining Stress Controller (LSC), which consists of multiple steel pipes in a concentric assembly (Moritz, 1999). Figure 23 shows the LSC as an integral part of the support, installed in the slots of a shotcrete lining and between stell ribs with frictional sliding joints. To demonstrate the effectiveness of the new system in comparison with a conventional support in practice, a 100 m long profile enlargement in squeezing rock was excavated in the Austrian Semmering railway tunnel (Figures 24 and 25).

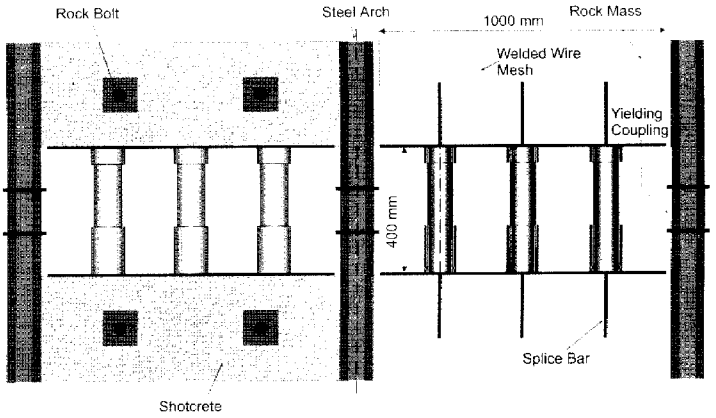

Figure 23: LSC units installed between lining segments (Moritz, 1999)

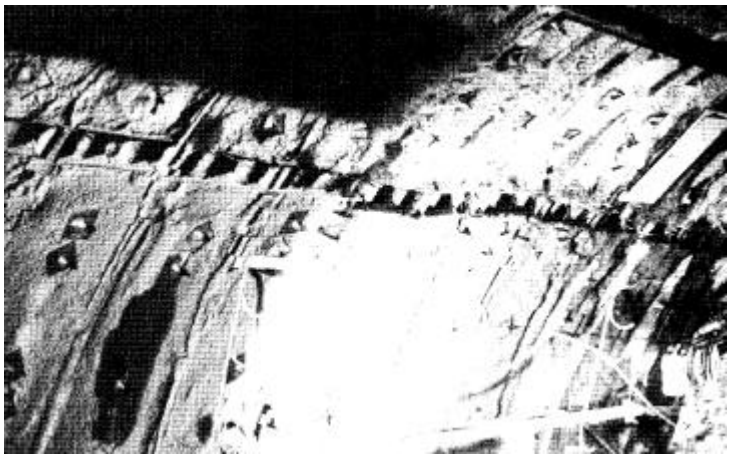

Figure 24: Improved support system with 150 mm deformed LSCs between the lining "segments" (Moritz, 1999)

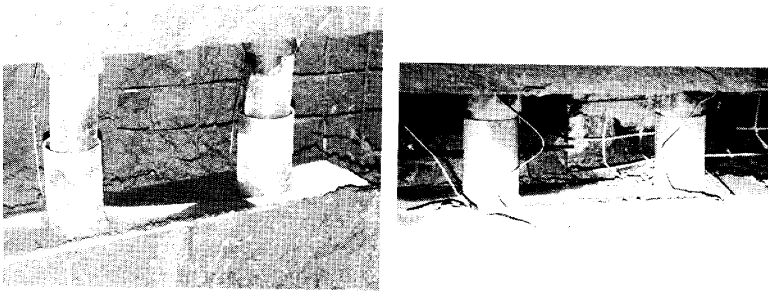

Figure 25: LSC A/I type unit installed in deformation slots before deformation (left) and after deformation (right) (Moritz, 1999)

3.3 Mechanised excavation

The use of Tunnel Boring Machines (TBM's) in squeezing rock conditions is characterized by a certain degree of difficulty. It is generally agreed at the present stage that experience and technology have not progressed far enough to recommend without some reservations machine excavation in such conditions. The major difficulties can be listed as follows:

- instability of the face;
- relative inflexibility in the excavation diameter;
- problems with the thrust due to reduced gripper action, for gripper type machines;
- difficulty to control the direction of the machine, in soft or heterogeneous ground.

Generally, instability of the face is felt not to be a problem because, when the machine is not moving ahead, the presence of the cutting head is sufficient to provide some form of face support. If the machine is advancing, any tendency to instability at the face is likely to be overcome as any squeezing is excavated as part of the cutting process. However, this is not necessarily true in severe squeezing conditions when face extrusion may become important and it is difficult if not impossible to control it. At the same time there are conditions that could become critical such as when the machine is heading perpendicularly to the stratification or in case of bed separation and buckling.

The problems associated with excessive deformations of the tunnel during excavation in squeezing conditions (Figures 26 and 27) are of great concern for both designers and contractors. As well known and will be discussed in the following, the type and magnitude of tunnel convergence are difficult to be anticipated precisely. At the same time, the choice of the excavation support measures to be adopted in order to stabilize the ground is not an easy task. Furthermore, the rate of advance, the quantity and type of support as well as the occurring deformations are interrelated and influence each other.

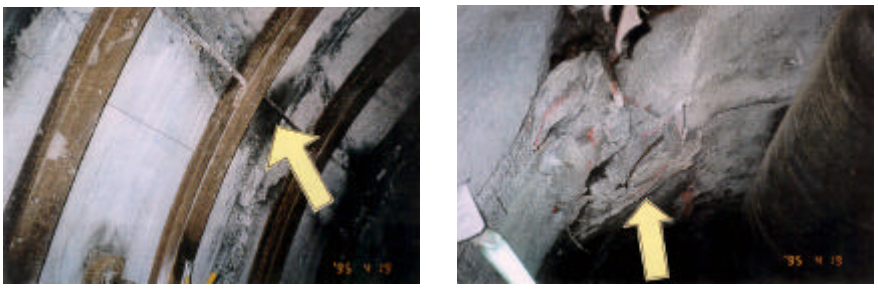

Figure 26: Damaged tunnel lining in the Pinglin pilot tunnel

Figure 27: Sheared lining in the Inntal tunnel (Schubert, 2000)

As discussed by Schubert (2000), the relationship between rate of advance and tunnel convergence can be quantified as shown in Figure 28, where the rate of advance was varied from 1 m/day to 30 m/day. The ultimate radial displacement computed for a typical case of squeezing behaviour is 300 mm. It is found that the radial displacement between the face and 10 m behind the face varies between 37 mm for an advance rate of 30 m/d and 83 m for an advance rate of 1 m/d. Therefore, the danger of TBM blockage in a squeezing zone (i.e. a fault zone) decreases with increasing advance rate. On the other hand nobody can guarantee that high advance rates can be maintained throughout a fault zone. Inflow of water, advancing face, overbreak, or machine breakdowns can bring the TBM to a stop. The still ongoing displacements then may squeeze the machine, making a restart difficult if not impossible.

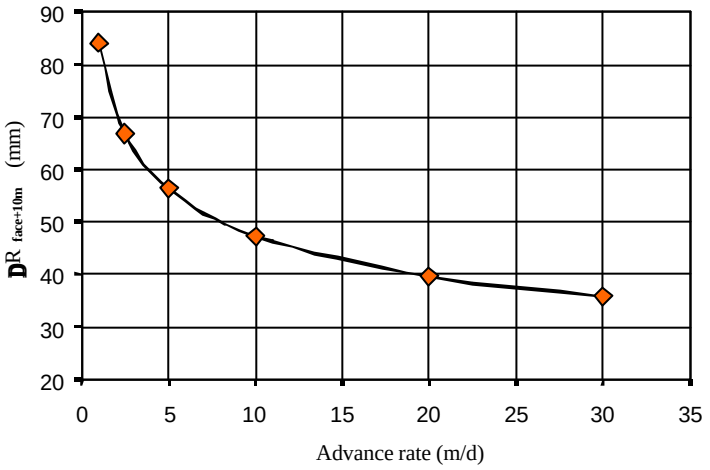

Figure 28: Relationship between advance rate and tunnel closure ten metres behind the face for different advance rates (Schubert, 2000)

A question open to debate when mechanised excavation is to be used and squeezing rock conditions are expected to be encountered along the tunnel length is the type of machine to be adopted, i.e. shielded or not shielded TBM's? Shielded TBM's are notoriously sensitive to rapid convergences and to the risk of blockage by converging rock, if special precautions are not taken. For the open TBM's, whenever large convergences occur in a short time and if these are associated with instabilities, as observed in situ in a number of cases, problems of support installation and gripping may occur, hampering the progress of excavation.

In order to cope with these problems, for most TBM's one foresees the possibility of increasing the diameter of the cutter head (overcutting), with the aim to be able to adjust the gap between the shield and the excavation contour from the

usual value of 6-8 cm to 15-25 cm (Figure 29). Radial overcut can be easily handled by open TBM's; for shielded TBM's lifting of the centreline of the cutter head with respect to the centreline of the shield is necessary in order to compensate convergences (Voerckel, 2001).

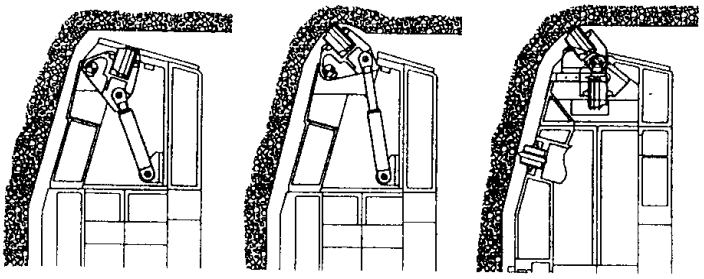

Figure 29: Solution for radial overcut by increasing the excavation diameter (Voerckel, 2001)

A TBM which has been developed to cope with squeezing conditions which are expected to be not too severe is shown in Figure 30. The technical provision adopted comprises an outershield (Walking Blade Shield) with parallel blades that are supported on hydraulic rams and can move independently in both axial and radial directions. This makes it possible to accommodate some radial deformation of the tunnel perimeter as the machine advances.

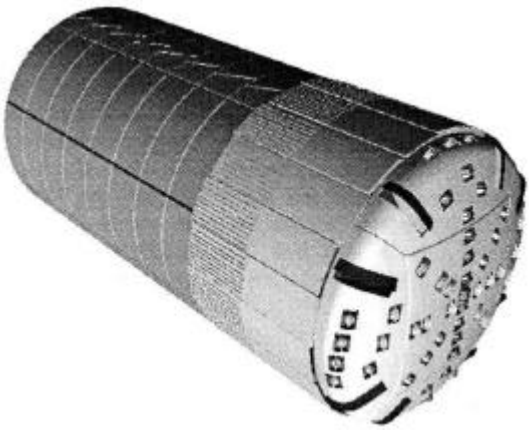

Figure 30: Walking Blade Shield (Robbins, 1997)

4. Analysis of rock mass response

Methods for analysis of tunnels in squeezing rock conditions need to consider:

- the onset of yielding within the rock mass, as determined by the shear strength parameters relative to the induced stress
- the time dependent behaviour.

An additional requirement is the estimate of the support pressure which is able to control the extent of the yielding zone around the tunnel and the resulting deformations. This poses considerable difficulties when the rock mass strength s_{cm} relative to the in situ stress p_0 is low and complex support/excavation sequences are envisaged in order to stabilize the tunnel during construction.

It is the purpose of this Chapter to address the methods (closed form solutions and numerical analyses) that are used at the design and analysis stage, with consideration given to the behavioral models which are generally introduced in order to represent the response of the rock mass surrounding the advancing tunnel. In all cases, a word of caution is needed when applying these methods to practical tunnel design in squeezing rock conditions. The difficulty is associated with the assessment of the rock mass properties, as the input data are often not available, inadequate or unreliable.

4.1 Closed form solutions

The usual approach is to assume the tunnel to be circular and to consider the rock mass subjected to a hydrostatic in situ state of stress, in which the horizontal and vertical stresses are equal. If the attention is payed to the rock mass response to excavation, which is described by the "ground reaction curve" or "rock characteristic line", one can plot the relationship between the support pressure p_i and the displacement u_r of the tunnel perimeter as shown in Figure 31.

4.1.1 Elasto-plastic solutions

If the rock mass is assumed to behave as an elasto-plastic-isotropic medium, the following models can be used (Figure 32):

- elastic perfectly plastic (1)
- elasto-plastic, with brittle behaviour (2)
- elasto-plastic, with strain softening behaviour (3).

A summary of the available closed form solutions for a circular tunnel in an elasto-plastic medium is given by Brown et al. (1983), who also present a solution where the rock mass follows the Hoek-Brown yield criterion and is consid-

ered to dilate during failure. A comprehensive set of solutions of the elasto-plastic type has been given by Panet (1995), in his book on the "*Convergence – confinement method*". More recently, a mechanically rigorous elasto-plastic solution for the problem of unloading a cylindrical cavity in a rock mass that obeys the Hoek-Brown yield criterion has been given by Carranza-Torres and Fairhurst (1999).

If consideration is given to models derived specifically with the squeezing behaviour in mind, the solution due to Aydan et al. (1993) is to be mentioned. As shown in Figure 5, this solution introduces a four branch stress-strain curve with (i) a linear elastic behaviour up to peak strength, (ii) a perfectly plastic behaviour at peak strength, (iii) a gradual decrease of stress to residual strength with increasing strain, (iv) a perfectly plastic behaviour beyond residual strength.

- **Solutions for models (1) and (2)**

For models (1) and (2) the closed form solutions are briefly reported by giving the fundamental equations for calculation of the extent of the plastic zone around the tunnel (the radius R_{pl}) and the resulting tunnel deformation (radial displacement u_r).

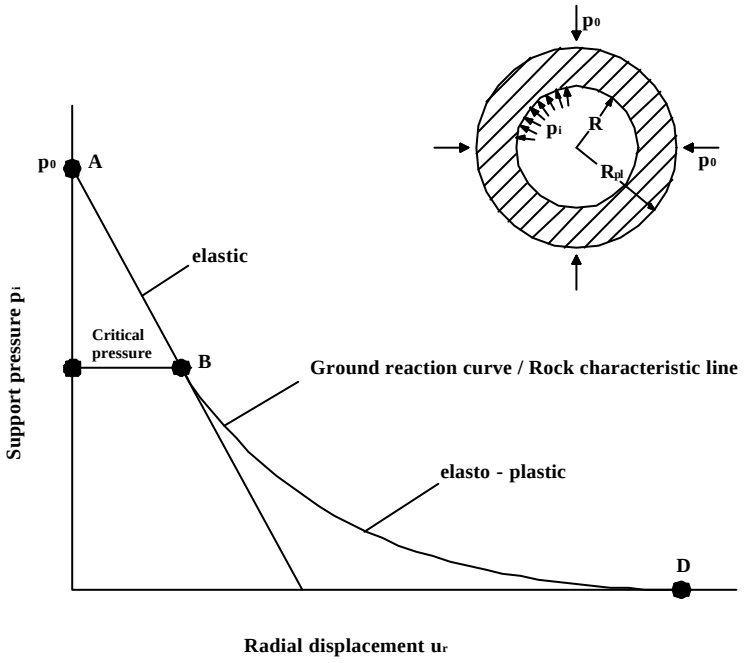

Figure 31: Axisymmetric tunnel problem: development of plastic zone around the tunnel and ground reaction curve/rock characteristic line

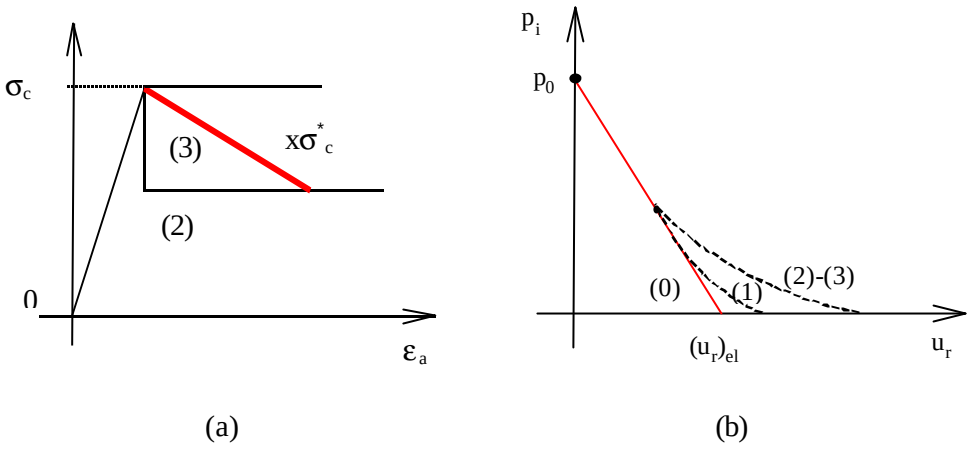

Figure 32: Elasto-plastic stress-stra in models generally used to derive the ground reaction curve: (a) stress strain laws; (b) ground reaction curves

(a) Let the rock mass have a Mohr-Coulomb yield criterion in which (a1) peak and residual strength coincide (the model is elastic perfectly plastic), or (a2) peak and residual strength are different (the model is elasto-plastic with brittle behaviour), Figure 32. The rock mass strength and deformation characteristics are defined in terms of:

- c_p, c_r = Cohesion (p and r stand for peak and residual values respectively)
- f_p, f_r = Friction angle (p and r stand for peak and residual values respectively)
- E = Young's modulus
- n = Poisson's ratio
- y = Dilation angle

One of the available solutions (Ribacchi and Riccioni, 1977) gives:

- for the radius of the plastic zone

$$R_{pl} = R \cdot \left\{ \frac{\left(p_0 + c_r \cdot \mathrm{cotg}\varphi_r\right) - \left(p_0 + c_p \cdot \mathrm{cotg}\varphi_p\right) \cdot \sin\varphi_p}{p_i + c_r \cdot \mathrm{cotg}\varphi_r} \right\}^{\frac{1}{N_f^{(r)} - 1}} \qquad (18)$$

with:

$$N_f^{(r)} = \frac{1 + \sin\varphi_r}{1 - \sin\varphi_r}$$

- for the critical pressure p_{cr}, defined by the initiation of plastic failure of the rock surrounding the tunnel

$$p_{cr} = p_0 \cdot (1 - \sin\varphi_p) - c_p \cdot \cos\varphi_p \qquad (19)$$

- for the radial displacement u_r in the elastic zone ($r \geq R_{pl}$)

$$u_r = \frac{1+\nu}{E} \cdot \left(p_0 - p_{cr}\right) \cdot \frac{R_{pl}^{\ 2}}{r} \tag{20}$$

- for the radial displacement u_r in the plastic zone ($R < r < R_{pl}$)

$$u_r = \frac{1+\nu}{E} \cdot \left\{ \frac{R_{pl}^{\ K'+1}}{r^{K'}} \cdot \left(p_0 + c_p \cdot \operatorname{cotg}\varphi_p\right) \cdot \sin\varphi_p + \left(p_0 + c_r \cdot \operatorname{cotg}\varphi_r\right) \cdot \left(1 - 2 \cdot \nu\right) \cdot \left(\frac{R_{pl}^{K'+1}}{r^{K'}} - r \right) - \frac{\left[1 + N_f^{(r)} \cdot K' - \imath \cdot \left(K'+1\right) \cdot \left(N_f^{(r)}+1\right)\right] \cdot \left(p_i + c_r \cdot \operatorname{cotg}\varphi_r\right)}{\left(N_f^{(r)} + K'\right) \cdot R^{N_f^{(r)}-1}} \cdot \left(\frac{R_{pl}^{N_f^{(r)}+K'}}{r^{K'}} - r^{N_f^{(r)}} \right) \right\} \tag{21}$$

with:

$$K' = \frac{1+\sin\psi}{1-\sin\psi}.$$

For the radial pressure p_i greater than p_{cr} (i.e. when the support pressure is greater than the critical value), the rock mass is in elastic conditions and equation (20) allows one to compute (for $r = R = R_{pl}$) the elastic portion of the characteristic line (Figure 31). For the radial pressure p_i smaller than p_{cr}, the characteristic line is given by (21) for $r = R$ and is concave upwards as shown in Figure 31.

(b) Let the rock mass have a Hoek-Brown yield criterion in which (a1) peak and residual strength coincide (the model is elastic perfectly plastic), or (a2) peak and residual strength are different (the model is elasto-plastic with brittle behaviour), Figure 32. The rock mass strength and deformation characteristics are defined in terms of:

σ_{ci} = uniaxial compressive strength of the intact rock;

m_p, m_r, s_p, s_r = Hoek-Brown constants;

according to Brown et al. (1993), the computations can be performed by the following equations:

- for the radius of the plastic zone

$$R_{pl} = R \cdot \exp\left[N - \frac{2}{m_r \cdot \sigma_{ci}} \sqrt{m_r \cdot \sigma_c \cdot p_i + s_r \cdot \sigma_c^2} \right] \tag{22}$$

$$M = \frac{1}{2} \cdot \sqrt{\left(\frac{m_p}{4} \right)^2 + \frac{m_p \cdot p_o}{\sigma_{ci}} + s_p} - \frac{m_p}{8} \tag{23}$$

$$N = \frac{2}{m_r \cdot \sigma_{ci}} \cdot \sqrt{m_r \cdot \sigma_{ci} \cdot p_o + s_r \cdot \sigma_{ci}^2 - m_r \cdot \sigma_{ci}^2 \cdot M} \tag{24}$$

- for the critical pressure p_{cr}, defined by the initiation of plastic failure of the rock surrounding the tunnel

$$p_{cr} = p_0 - M \sigma_c \tag{25}$$

- for the radial displacement u_r in the elastic zone ($r \geq R_{pl}$)

$$u_r = \frac{1+\nu}{E} (p_o - p_{cr}) \frac{R_{pl}^2}{r} \tag{26}$$

- for the radial displacement u_r in the plastic zone ($R \leq r \leq R_{pl}$)

$$u_r = \frac{M \cdot \sigma_{ci} \cdot 2 \cdot (1+\nu)}{E \cdot (f+1)} \cdot \left[\frac{(f-1)}{2} + \left(\frac{R_{pl}}{r} \right)^{f+1} \right] \cdot r \tag{27}$$

where f is:

$$f = 1 + \frac{m_p}{2\sqrt{\frac{m_p p_{cr}}{\sigma_{ci}} + s_p}} \tag{28}$$

- **Example**

An example of a typical plot of a characteristic line under the assumption of elastic perfectly plastic behaviour is given in Figure 33, in conjunction with the thickness of the plastic zone ($R_{pl} - R$). The tunnel is 11.5 m in diameter and is subjected to a hydrostatic stress p_0 = 5 MPa. The rock mass follows the Mohr-

Coulomb yield criterion with f = 15°, c = 400 kPa, y = 15°. The rock mass modulus is 1.5 GPa.

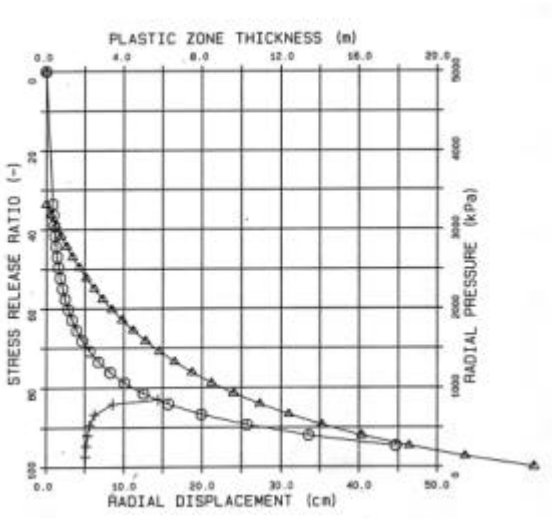

Figure 33: Example of "rock characteristic line" plot for a 11.50 m diameter tunnel. The in situ state of stress is isotropic, p_0 = 5 MPa. The rock mass failure is defined by the Mohr-Coulomb criterion (cohesion c = 0.4 MPa, friction angle f = 15°) with a dilatation angle y = 15°. The in situ deformation modulus E = 1.5 GPa. Also shown is the "support characteristic line", represented by a 25 cm thick shotcrete lining with steel ribs.

4.1.2 Time dependent response

The influence of the time-dependent mechanical properties of the rock mass on the response of a tunnel to excavation has been modeled by many authors using visco-elastic and visco-plastic constitutive equations. Ladanyi (1993) and Cristescu (1993) give a comprehensive presentation of the available solutions for simple tunnelling cases and models of behaviour:

- linear visco-elastic
- linear elastic - linear viscous
- linear elastic - non linear viscous
- elastic - visco-plastic.

(a) A typical simple example of analysis for a linear visco-elastic model consists in using the so called Maxwell model given in Figure 34, where an elastic spring and a viscous dashpot are put in series. In such a case, the radial displacement u_r at the tunnel contour (as for the closed form solutions previously discussed for the elasto-plastic case, the tunnel is circular and the rock mass is subjected to a hydrostatic state of stress) is given by:

$$u_r = \frac{(p_o - p_i)R}{2G}\left(1 + \frac{t}{T}\right) \tag{29}$$

where:

t = time

T = $\frac{\eta}{G}$, relaxation time.

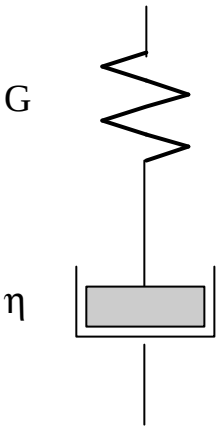

Figure 34: Maxwell linear visco-elastic model

If a linearly elastic lining (a ring) with stiffness K_s is installed at time t_s, the displacement u_r is:

$$u_r = \frac{p_0 R}{2G}\left(1 + \frac{t}{T}\right) + \frac{p_c R}{K_s} \tag{30}$$

with the pressure p_c on the same lining being given by:

$$p_c = p_0\left[1 - \exp\left(-\frac{t - t_s}{T\left(1 + \frac{2G}{K_s}\right)}\right)\right] \tag{31}$$

(b) Similarly, with reference to the linear Kelvin-Voigt visco-elastic model of Figure 35 one would obtain for u_r, when no lining is installed yet

$$u_r = \frac{(p_0 - p_i)R}{2G_0}\left[1+\left(\frac{G_0}{G_f}-1\right)\cdot\left(1-\exp\left(-\frac{t}{T}\right)\right)\right] \tag{32}$$

where:

$T = \frac{\varsigma_1}{G_1}$

$G_f = \frac{1}{G_0}+\frac{1}{G_1}$;

with the lining installed at time t_s, the following equations are obtained for u_r and p_c

$$u_r = \frac{p_0 \cdot R}{2 \cdot G_0}\cdot\left[1+\left(\frac{G_0}{G_f}-1\right)\cdot\left(1-\exp\left(-\frac{t_s}{T}\right)\right)\right]+\frac{p_c \cdot R}{k_s} \tag{33}$$

$$p_c = p_0 \times \left[\frac{1-\frac{G_f}{G_0}}{1+2\cdot\frac{G_f}{K_s}}\right]\exp\left(-\frac{t_s}{T}\right)\cdot\left[1-\exp\left(\frac{2+\frac{K_s}{G_f}}{2+\frac{K_s}{G_0}}\right)\cdot\left(-\frac{t-t_s}{T}\right)\right] \tag{34}$$

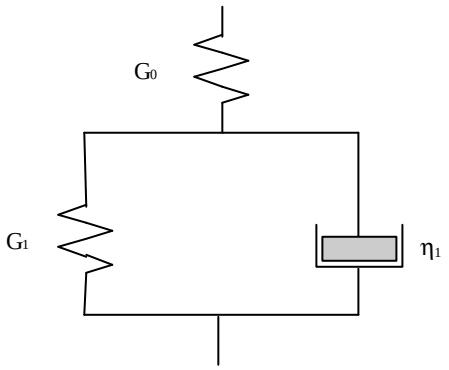

Figure 35: Kelvin-Voigt visco-elastic model

(c) If consideration is given to squeezing behaviour, the visco-elastic models above, where the assumption is that the time effect can be separated from the

stress effect in the general creep formulation, are not appropriate. Therefore, models of the elastic-visco-plastic type should be used.

A simple model of interest, due to Sulem et al. (1987), allows the analysis of time-dependent stress and strain fields around a circular tunnel in a creeping rock mass with plastic yielding. Although valid for a monotonic stress path, this model is well suited for the problem considered and allows a closed form solution for the computation of the time-dependent convergence.

As discussed by Sulem (1994), the total strain ε is obtained by adding together the time-independent elastic strain e^{e} and the time-dependent inelastic strain e^{ne}

$$e = e^{e} + e^{ne}$$

where:
$e^{ne} = e^{p} + e^{c}$ for e^{p} = plastic strain and e^{c} = creep strain.

The creep strain is written as an explicit function of stress s_{ij} and of time t as an explicit parameter

$$e^{c} = g(s_{ij}) f(t) \tag{35}$$

where f is an increasing function of time with $f(0) = 0$ and $\lim_{t \to \infty} f(t) = 1$.

If $g(s_{ij})$ is taken as a linear law (the most appropriate form for rock is a power law) and the creep strain is assumed to depend only on the deviatoric stress and to occur at constant volume, the radial strain e_r^c and the tangential strain e_q^c can be written as (Sulem, 1994)

$$e_r^c = -\frac{s_q - s_r}{4G_f} f(t) \tag{36}$$

$$e_q^c = \frac{s_q - s_r}{4G_f} f(t) \cdot \tag{37}$$

where G_f is a creep modulus.

Let the rock mass follow a Mohr-Coloumb yield criterion in which peak and residual strength coincide ($c_p = c_p = c$; $f_p = f_r = f$), and the deformations subsequent to yielding occur at constant volume ($y = 0$). As demonstrated by Sulem et al. (1987), under these conditions the linearity of the creep law with stress leads for the stress field around the tunnel to the same results as for the simple elastic perfectly plastic model. The plastic radius R_{pl} and the critical pressure

p_{cr}, defined by the initiation of plastic failure of the rock around the tunnel, are given by the same expressions as (18) and (19).

The radial displacement at the tunnel wall is:
for $p_i > p_{cr}$

$$u_r = \frac{p_0 R}{2G}\left(1 + \frac{G}{G_f} f(t)\right) \cdot \tag{38}$$

for $p_i < p_{cr}$

$$u_r = \frac{p_0 R}{2G}\left(\frac{R_{pl}}{R}\right)^2 \left(1 + \frac{G}{G_f} f(t)\right) \lambda_e \,. \tag{39}$$

where:

$$\lambda_e = \sin\varphi + \frac{c\cos\varphi}{p_0} \tag{40}$$

5. Rock-support interaction analysis

5.1 Rock mass response

The closed form solutions described above allow one to obtain the rock "characteristic line" for a circular tunnel and different rock mass response models, under the assumption of isotropy for both the rock mass and the initial state of stress. These solutions can be very useful in order to gain insights into tunnel behaviour when the excavation takes place in rock masses which exhibit squeezing conditions.

As recently shown by Hoek (1998, 1999a), dimensionless plots can be derived from the results of parametric studies where the influence of the variation in the input parameters has been studied by a Monte Carlo analysis, under the assumption of elastic perfectly plastic behaviour of the rock mass, with zero volume change. Two of such plots are given in Figures 36 and 37, which were unloaded directly from Dr. Evert Hoek's course notes available on the website: www.rocscience.com (Hoek, 1999a).

Figure 36 gives a plot of the ratio of the plastic zone radius to tunnel radius and Figure 37 shows the corresponding ratio of tunnel deformation to tunnel radius versus the ratio of rock mass strength to in situ stress, for the condition of zero support pressure (p_i = 0). As already noted in Chapter 2, once the rock mass strength falls below 20% of the in situ stress level ($s_{cm} \leq 0.2\ p_0$), the plastic

zone size increases very rapidly with a corresponding substantial increase in deformation. It is clear that if this stage is reached, unless the deformations are controlled, collapse of the tunnel is likely to occur.

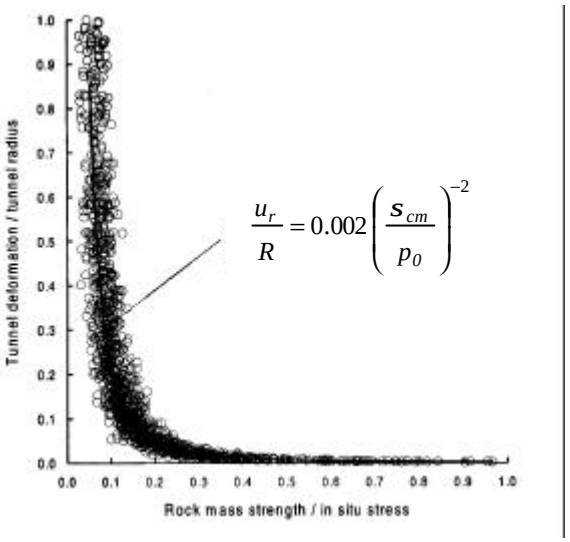

Figure 36: Tunnel deformation versus ratio of rock mass strength to in situ stress for weak rock masses (Hoek, 1999a)

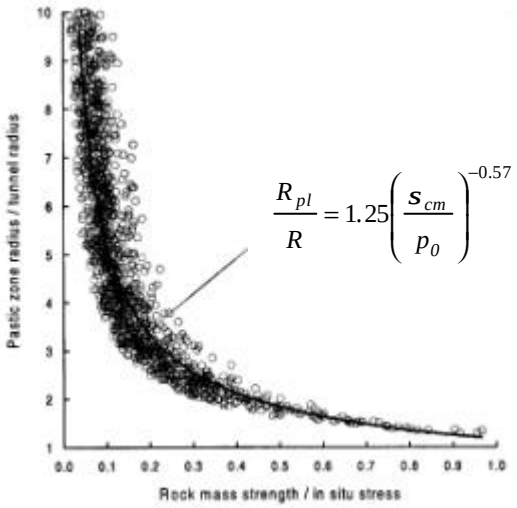

Figure 37: Relationship between size of plastic zone and ratio of rock mass strength to in situ stress for weak rock masses (Hoek, 1999a)

5.2 Support response

In order to complete the rock-support interaction analysis, the support behaviour is to be considered in detail by determining the "support characteristic line" which relates the confining pressure acting on the support to its deformation. Knowing the radial displacement u_{r0} that has occurred before the support is installed at a known distance from the face, the equilibrium solution for the rock support interaction analysis is given by the intersection of the "rock characteristic line" and the "support characteristic line". This is the essence of the so called "convergence-confinement method" (Figure 38).

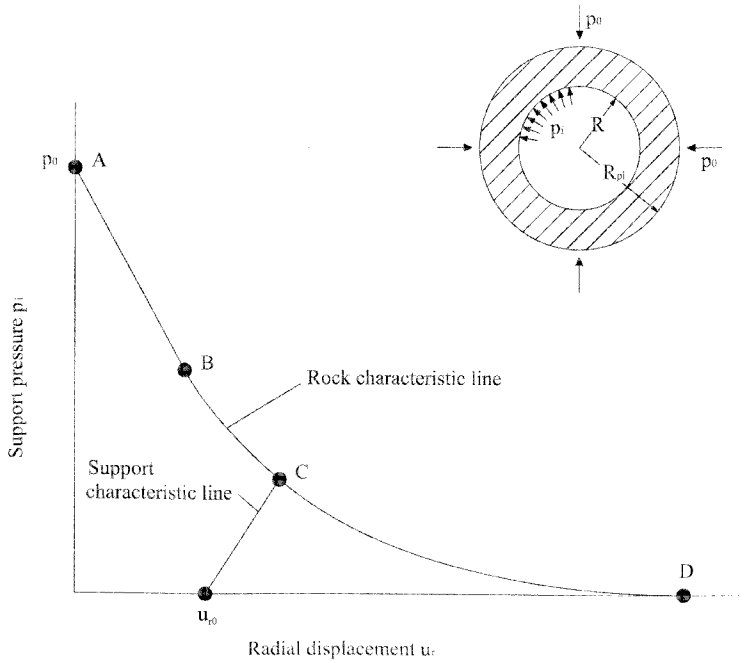

Figure 38: Axisymmetric tunnel problem: rock characteristic line and support characteristic line

The deformation that has occurred before the support is installed is not easy to be determined as complex three-dimensional stress analyses are required in order to account for the influence of the face, the method and sequence of excavation, the possible installation of pre-supports ahead of the face, etc. In simple cases, guidelines have been given by Panet and Guenot (1982), Bernaud (1991) and Panet (1995). In more complex conditions, it is advisable to use monitoring results of instrumentation installed before excavation and back analysis, as discussed in Chapter 6.

The "support characteristic line" can be computed by a set of equations (Hoek and Brown, 1980; Brady and Brown, 1985) which allow one to determine the stiffness k_i and the maximum support pressure $p_{i\,max}$ for typical support systems. For sake of completeness some of these equations are written below.

- **Concrete or shotcrete lining**

- *Support stiffness*

$$k_c = \frac{E_c\left(r_i^2 - (r_i - t_c)^2\right)}{r_i(1+\nu_c)\left((1-2\nu_c)r_i^2 + (r_i - t_c)^2\right)}. \tag{41}$$

- *Maximum support pressure*

$$p_{sc\,max} = \frac{1}{2}\sigma_{c,c}\left[1 - \frac{(r_i - t_c)^2}{r_i^2}\right]. \tag{42}$$

where:
E_c = Young's modulus of concrete or shortcrete;
ν_c = Poisson's ratio of concrete or shotcrete;
t_c = lining thickness;
r_i = internal tunnel section;
$\sigma_{c,c}$ = uniaxial compressive strength of concrete or shortcrete.

- **Steel sets embedded in shotcrete**

- *Support stiffness*

$$(k_s)^{-1} = \frac{S_{r_i}}{E_s A_s} + \frac{d}{E_c r_i} \tag{43}$$

- *Maximum support pressure*

$$p_{sc\,max} = \frac{A_s \cdot \sigma_s}{r_i \cdot S}. \tag{44}$$

where:
E_s = Young's modulus of steel;
A_s = cross sectional area of steel set;
S = steel set spacing along tunnel axis;
d = mean overbreak filled with shotcrete;
σ_s = yield strength of steel.

- **Ungrouted mechanically or chemically anchored rock bolts**

- *Support stiffness*

$$(k_b)^{-1} = \frac{S_c \cdot S_l}{r_i}\left[\frac{4l}{\pi d_b^2 E_b} + Q\right] \tag{45}$$

- *Maximum support pressure*

$$p_{bc\,max} = \frac{T_{bf}}{s_c \cdot S_l} \cdot \tag{46}$$

where:
S_c = circumferential bolt spacing;
S_l = longitudinal bolt spacing;
l = free bolt length;
E_b = Young's modulus of bolt;
d_b = bolt diameter;
Q = load-deformation constant for anchor and head (as obtained on the bolt load-extension curve of a pull-out test);
T_{bf} = bolt ultimate failure load.

It is also to be mentioned that estimates of support capacities for a variety of different systems (steel sets, lattice girders, rock bolts and dowels, concrete and shotcrete linings) for a range of tunnel sizes have been recently published by Hoek (1999). A word of caution is appropriate by saying that, in all cases, the support is always assumed to act over the full perimeter of the tunnel, including the invert (i.e. a closed ring condition is therefore assumed to hold true).

5.3 Numerical analyses

The use of numerical analyses is advisable in cases where the s_{cm} / p_0 ratio is below 0.3, and it is highly recommended if this ratio falls below about 0.15, when the stability of the tunnel may become a critical issue. Significant advantages are envisaged by using numerical analyses at the design stage, when very complex support/excavation sequences, including pre-support/stabilisation measures are to be adopted, in order to stabilize the tunnel during construction (see Chapter 3).

Very powerful computer codes have been developed and are now available for the stress and deformation analysis of tunnels. It is therefore possible to develop

reliable predictions of tunnel behaviour, provided a proper understanding of the real phenomena as observed in practice is available. With respect to closed-form solutions, anisotropic in situ stress fields can now be considered, together with multiple excavation stages, the influence of face advance, and the important three-dimensional conditions which occur in the immediate vicinity of the face, the consequence of liner placement delay, etc..

5.3.1 Continuum approach

If we remain with the equivalent continuum approach, where the rock mass is treated as a continuum with equal in all directions input data for the strength and deformability properties, which define a given constitutive equation for the rock mass: elastic, elasto-plastic, visco-elastic, elastic-visco-plastic the domain methods, which include the finite element (FEM) and the finite difference (FDM) methods, can be used. An example of a typical stress-deformation analysis of a circular tunnel, for the same properties for the rock mass as shown in Figure 33, is given in Figure 39, where the confining pressure p$_i$ is set equal to 0.8 MPa, which is the equilibrium solution for the rock-support interaction analysis. The results obtained by the FLAC code (version 3.4), Itasca (1998), compare reasonably well with the closed-form solution as shown in Table 4.

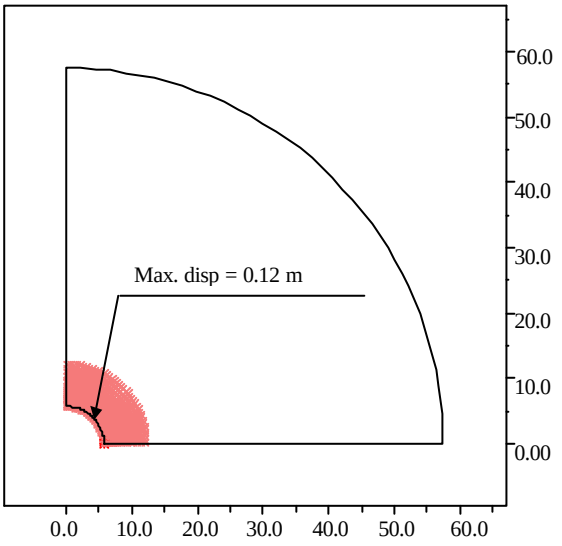

Figure 39: Stress deformation analysis of a circular tunnel by the FLAC code. The example shown is described in Figure 33

Table 4: comparison of results for characteristic line calculation and FDM solution for the example shown in Figure 38

	characteristic line	FDM solution
radial displacement u_r (cm)	14.00	12.12
plastic radius R_{pl} (m)	11.75	12.40

One of the obvious advantages of numerical methods in the analysis and design of tunnels in squeezing rock conditions is the use of more complex stress-strain models for the rock mass such as the strain softening behaviour and time dependent behaviour, which can be implemented with both FEM and FDM. Some examples will be discussed in the following for purpose of illustration. Although this is obviously not a requirement as for the closed form solutions previously discussed, the tunnel is considered to be circular and subjected to a hydrostatic stress field.

- **Elasto-plastic models**

For example, consider a 8 m diameter tunnel to be excavated in a weak rock mass at depth of up to 800 m below surface (p_0 = 20 MPa). The uniaxial compressive strength of the intact rock s_{ci} is equal to 55 MPa and the m$_i$ parameter for the Hoek-Brown criterion has been determined to be 12 ([5]).

The strength and deformation characteristics of the rock mass are estimated by means of the procedure described by Hoek and Brown (1997). For a mean value of the GSI index taken equal to 40, by fitting by linear regression eight equally spaced values pertaining to the Hoek-Brown rock mass criterion, in the range $0 < s'_3 < 0.25\ s_{ci}$, the c and ϕ peak parameters for the rock mass can be obtained. Accordingly, the post-peak characteristics are estimated by reducing the GSI value to a lower value which characterizes the broken rock (GSI = 30).

The assumed rock mass parameters are as follows:

uniaxial compressive strength	s_{cm}	=	7.7 MPa
deformation modulus	E	=	6.0 GPa
Poisson's ratio	n	=	0.3
peak cohesion	c_p	=	2.0 MPa
peak friction angle	f_p	=	30°
residual cohesion	c_r	=	1.0 MPa
residual friction angle	f_r	=	15°

([5]) The intact rock mass parameters used in this example pertain to the so called "Briançonnaise coal measure zone" along the Moncenise tunnel, Lyon-Torino high-speed railway line. It is noted that for the rock mass under consideration (s_{cm} = 7.7 MPa) at 800 m depth (p_0 = 20 MPa), the ratio s_{cm} / p_0 is equal to 0.35 approximately, which makes one anticipate "minor squeezing problems" in this section of the tunnel, at least based on the data presently available.

Two dimensional analyses were carried out by the FLAC code. For the purpose of this example, the following stress-strain laws were considered:

- elastic perfectly plastic ((1) in Figure 32; for $c_p = c_r$, $f_p = f_r$, $y = 0°$)
- elasto-plastic with brittle behaviour ((2) in Figure 32; with the rock mass parameters listed above and $y = 0°$)
- Aydan model (Figure 5, ε_s=0.008, ε_f=0.0158).

The support pressure p_i was always assumed to be 0 MPa.

A plot of the yielding zones around the tunnel and the corresponding displacements for models (1) and (2) is shown in Figure 40 (a) and (b). The calculated displacements at the tunnel contour and the plastic radius are given in Table 5, where also reported are the results for the Aydan model. It is noted that, for the overburden condition under consideration, the elasto-plastic stress-strain law with brittle behaviour shows a tendency to overestimate both the displacements and the extent of the plastic zone.

Table 5: Results of 2D analyses

analysis	2D	
	R_{pl} (m)	u_{max} (cm)
perfectly plastic	7.0	3.8
brittle	18.7	41.0
Aydan	7.7	4.7

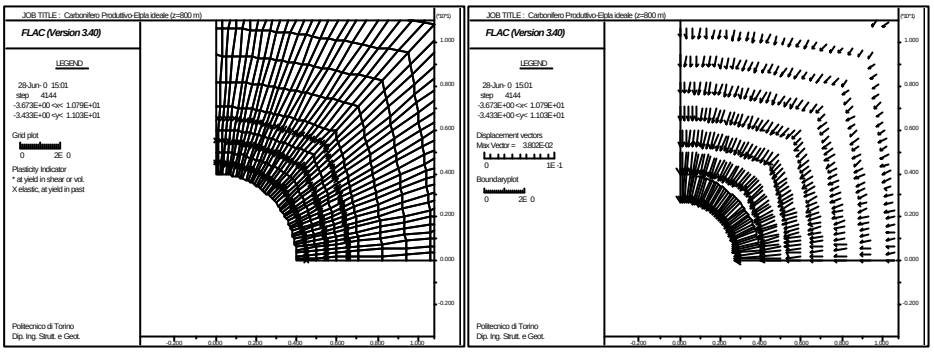

(a)

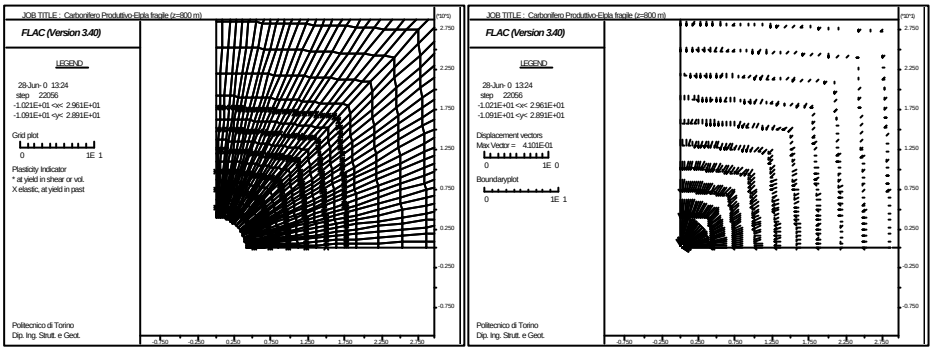

(b)

Figure 40: Results of 2D analyses for different models of behaviour for the rock mass ((a) elastic perfectly plastic; (b) elasto-plastic with brittle behaviour; showing the extent of the plastic zone and the displacements around the tunnel (see text for input data)

An additional point of interest for the calculations carried out is the stress distribution around the tunnel, as dependent on the stress-strain laws assumed to simulate squeezing. Figure 41 shows the maximum (s_1) and minimum (s_3) principal stresses at an increasing distance from the tunnel contour for the elastic perfectly plastic (dashed line) and Aydan stress-strain law (continuous line). The Aydan stress-strain law shows a wider zone where the rock mass is at yield, with an increase in the plastic radius of 1 m approximately.

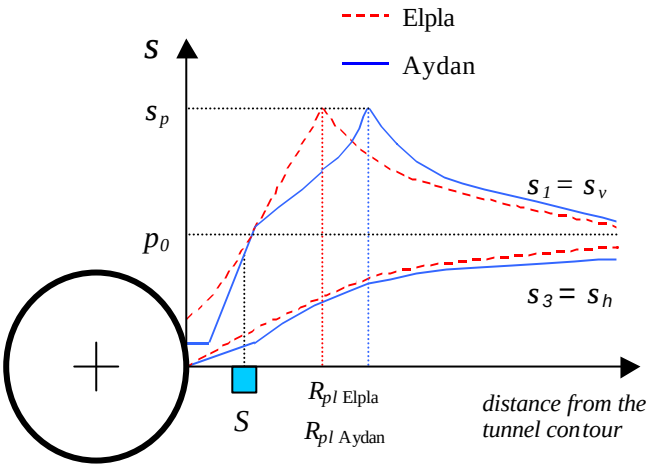

Figure 41: Stresses at different distances from the tunnel contour for elastic perfectly plastic and Aydan stress-strain law

- **Time dependent response**

For example, take a 6 m diameter tunnel located in a weak rock mass a depth of 300 m below surface (p_0 = 7.5 MPa). Based on the estimated *GSI* index equal to 30, the assumed Mohr-Coulomb rock mass parameters are as follows:

Deformation modulus	E	=	4.5 GPa
Poisson's ratio	n	=	0.25
Cohesion	c	=	0.15 MPa
Friction angle	f	=	28°.

Two-dimensional analyses were carried out by the FLAC code. For the purpose of this example, the following time dependent models of behaviour are considered:

- linear visco-elastic
- elastic visco-plastic.

Also considered in the example is the presence of a 45 cm thick concrete circular lining which is given a linear elastic behaviour with the following parameters:

Elastic modulus	E	=	31.0 GPa
Poisson's ratio	n	=	0.25.

In the numerical analyses the lining is simulated by using Beam type elements as available with the FLAC code.

(a) In order to compare with the closed form solutions previously given for the linear visco-elastic case, the first series of numerical analyses assume the Maxwell and Kelvin-Voigt models with the following parameters:

- Maxwell model

Shear modulus $G = 2.0$ GPa
Viscous coefficient $h = 6.0$ MPa · year.

- Kelvin-Voigt model

Shear modulus $G_0 = 2.0$ GPa
Shear modulus $G_1 = 2.0$ MPa · year.
Viscous coefficient $h_1 = 6.0$ GPa · year.

The results obtained are illustrated in Figures 42 and 43 for the Maxwell and Kelvin-Voigt model respectively. In each case the closed-form solutions (equations (29), (30) and (31), for the Maxwell model; equations (32), (33) and (34), for the Kelvin-Voigt model) are compared with the numerical results. In general this comparison is quite satisfactory for both the computed radial displacement and the lining pressure. In one case, for the Kelvin-Voigt model, the numerical solution appears to overestimate slightly the pressure value acting on the lining, at least for the first 6 years of loading.

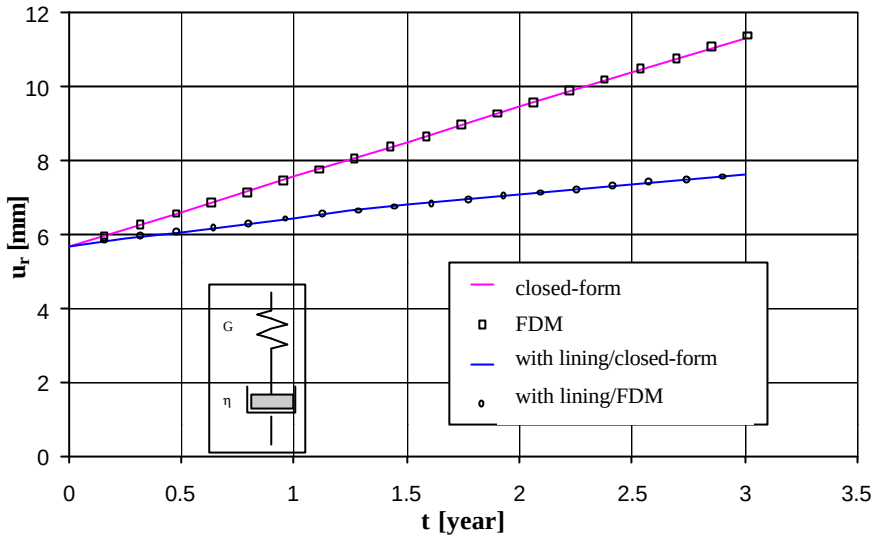

(a)

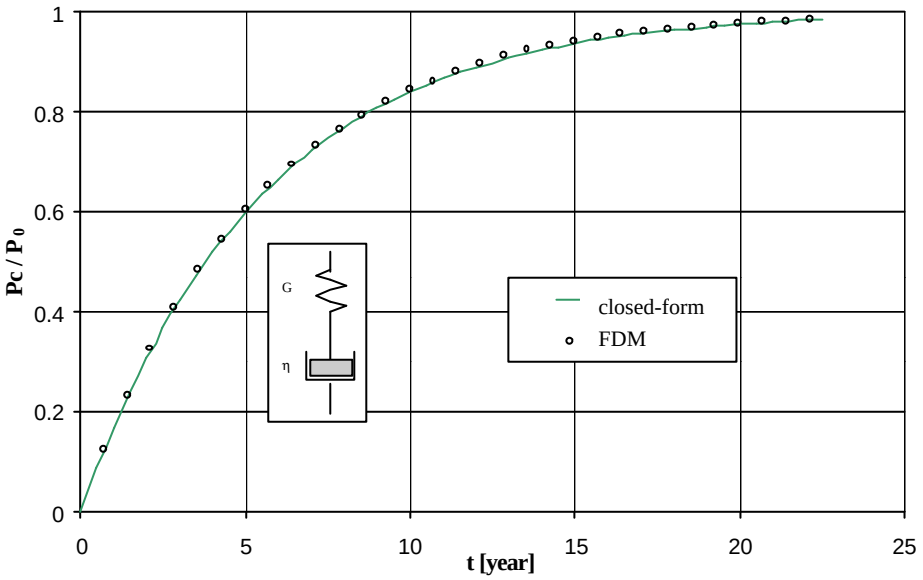

(b)

Figure 42: Comparison of closed-form solutions and Finite Difference Methods (FDM) results for the Maxwell visco-elastic models: (a) radial displacement; (b) lining pressure. Note: the lining is installed instantaneously at $t = 0$.

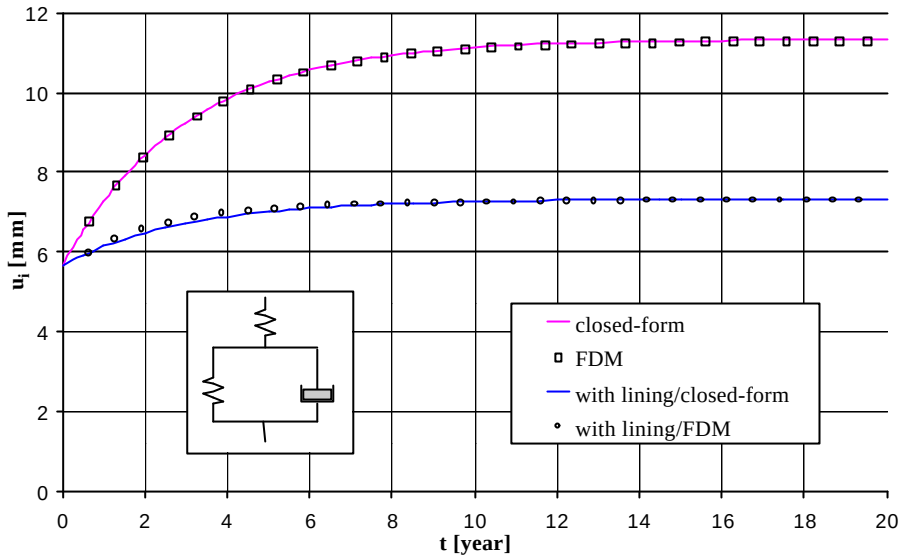

(a)

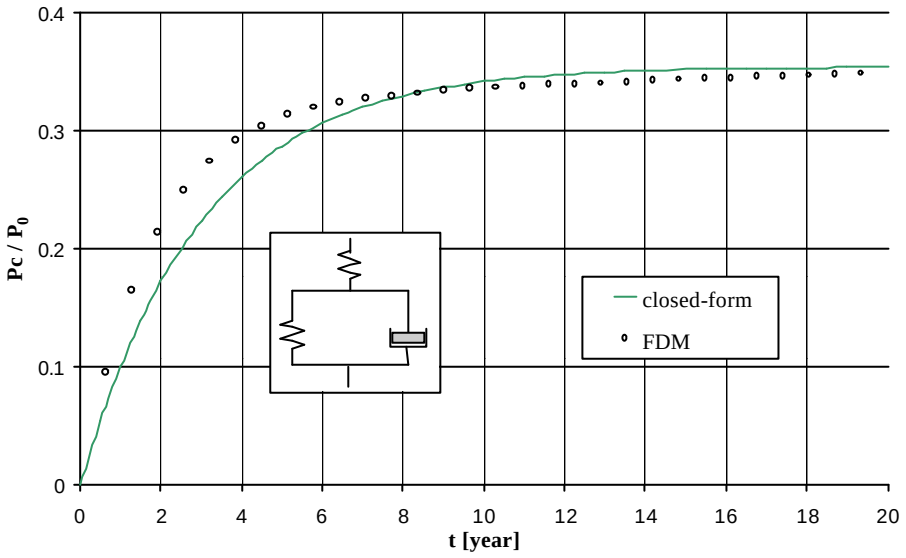

(b)

Figure 43: Comparison of closed-form solutions and Finite Difference Methods (FDM) results for the Kelvin-Voigt visco-elastic models: (a) radial displacement; (b) lining pressure. Note: the lining is installed instantaneously at $t = 0$

(b) For the elastic-visco-plastic case the calculations were performed with the Finite Difference Method only and the FLAC code. Considering that this model of behaviour is of great interest when dealing with squeezing rock conditions (Gioda and Cividini, 1996), the visco-elastic component is chosen to correspond to a Burger model (Kelvin model in series with a Maxwell model as shown in Figure 44), which gives a more representative time-dependent response for a rock mass than either the Maxwell or Kelvin-Voigt model. The plastic stress-strain law corresponds to a Mohr-Coulomb model.

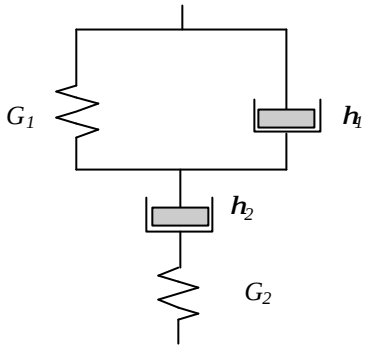

Figure 44: Burger visco-elastic model

The rock mass parameters according to a Mohr-Coulomb model are those given at the beginning of this example. The time dependent parameters for the Burger model are as follows:

- Kelvin model

Shear modulus G_1 = 2.0 GPa
Viscosity η_1 = 6.0 MPa · year.

- Maxwell model

Shear modulus G_2 = 2.0 GPa
Viscosity η_2 = 0.6 GPa · year.

The results obtained are illustrated in Figures 45 and 46. It is shown that the concrete lining, which is installed 2 months approximately following excavation, succeeds in controlling the tunnel deformation (Figure 45a) as it is being loaded significantly in a relatively short time (Figure 45b). In absence of any support pressure, the plastic radius is shown to increase versus time as shown in Figure 46; it is clear from the same figures that the presence of a stiff lining contributes to limit the extent of the plastic radius.

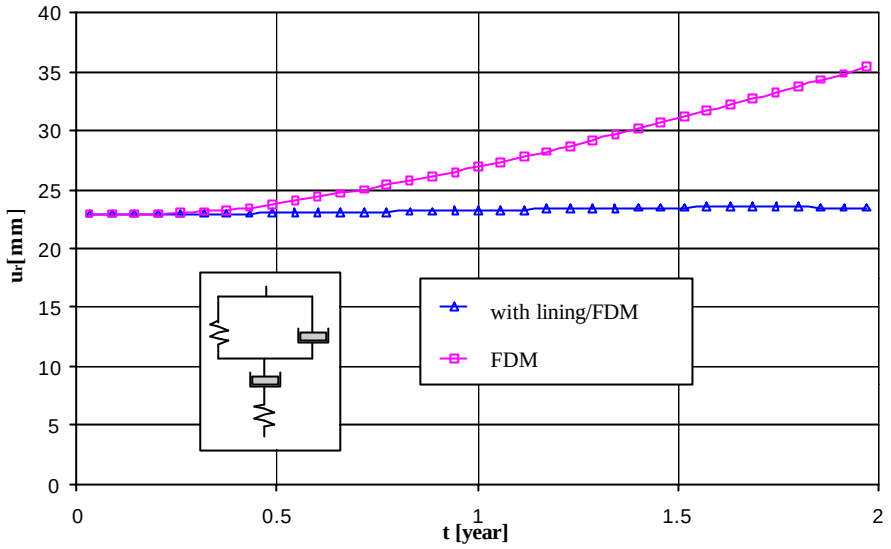

(a)

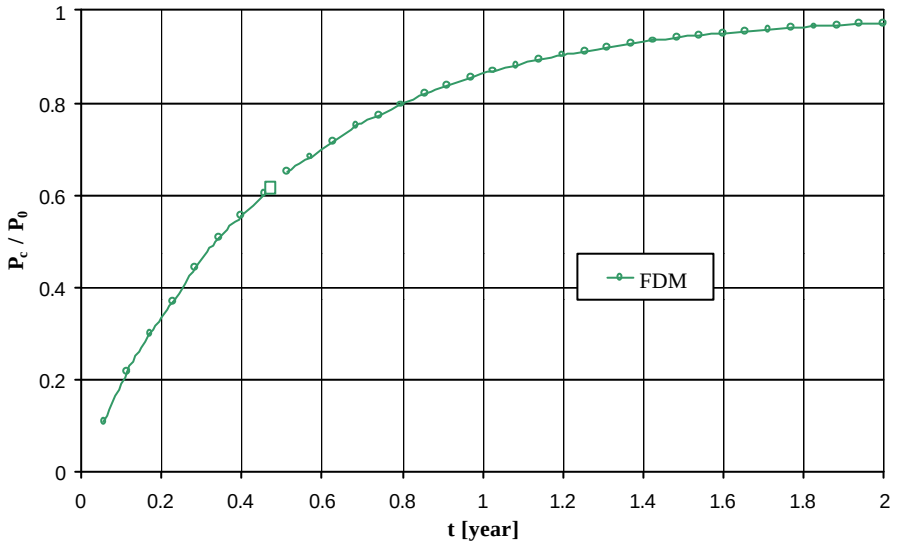

(b)

Figure 45: Finite Difference methods (FDM) results for the elastic visco-plastic models: (a) radial displacement; (b) lining pressure. Note: the lining is installed instantaneously at $t = 0$

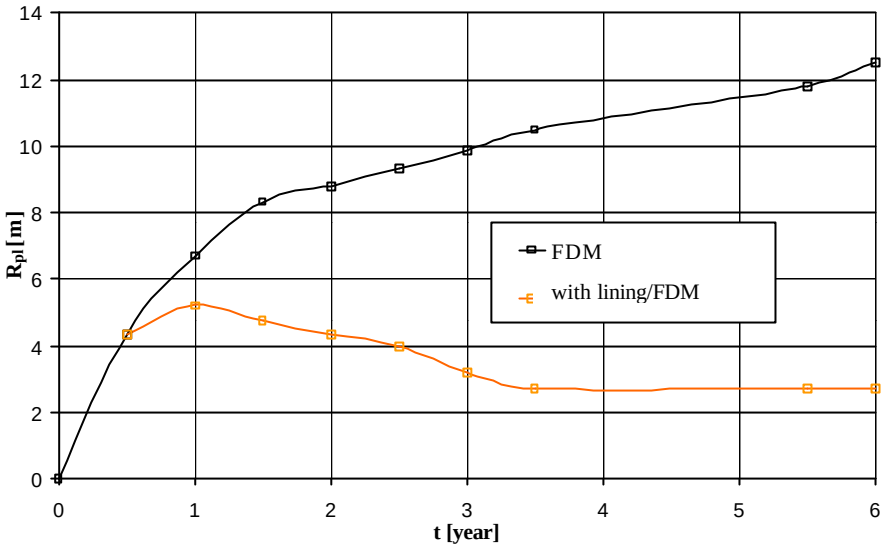

Figure 46: Computed plastic radius around the tunnel for the elastic-visco-plastic model

5.3.2 Discontinuum approach

In weak rock masses which exhibit a squeezing behaviour, the use of continuum representations of the medium subjected to excavation is reasonable. In general, the results obtained are applicable with success in practical tunnel design, provided that engineering judgement and precedent experience are used. However, there are cases where discontinuum modelling could be the most appropriate in order to analyze a given problem.

The example shown in Figure 47well illustrates this point of view. The rock mass is argillite, intersepted by beddings which strike nearly parallel to the tunnel axis. A nearly vertical discontinuity system is as well present. Both the bedding and the jointing are very closely spaced and persistent so that the rock mass is subdivided into very small blocks. The plot shown in Figure 47 (a) gives a DFN (Discrete Feature Network) model which was created in order to simulate the rock mass behaviour by using the Distinct Element Method and the UDEC code, Itasca (1998).

The joints are assumed to be Mohr-Coulomb joints, i.e. elastic perfectly plastic. The blocks are treated as an elasto-plastic material which follows the Mohr-Coulomb criterion. The properties of rock blocks and joints are listed in Table 2. The in situ state of stress is anisotropic with a vertical stress of 5 MPa and the stress ratio (horizontal to vertical stress) equal to 1.5.

The results obtained are plotted in Figure 47 (b) to (d) by giving: Figure 47 (b), the displacement vectors; Figure 47 (c), the open zones; Figure 47 (d) the yielded blocks. It is shown that, although the rock mass is very weak and of poor quality, as expected on the basis of the properties above, the orientation of discontinuities plays a very important role on the onset and development of stress and deformations around the tunnel, and therefore also on the squeezing behaviour.

Table 6: Material and joint properties used in the FDN model

material properties		joint properties	beddings	joints
E (GPa)	5	K_n (GPa/m)	10	10
n	0.25	K_s(GPa/m)	1	1
c (MPa)	5	c (kPa)	10	50
f (°)	30	f (°)	20	35

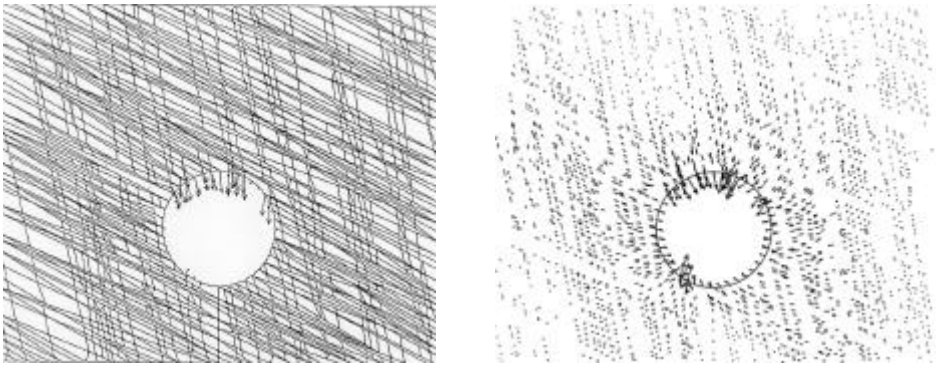

(a) (b)

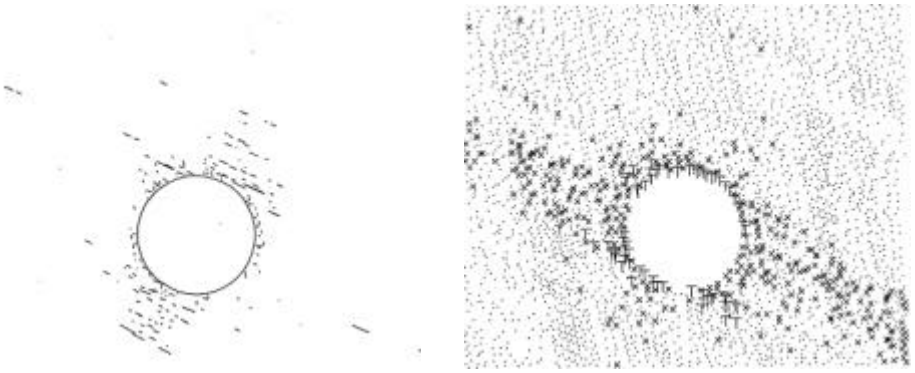

(c) (d)

Figure 47: Results of a DFN model representing a 11 m diameter tunnel in argillite. (a) DFM model; (b) Displacement distribution (maximum value 0.159 m); (c) Open Zones; (d) Failure Zone

5.3.3 Influence of 3D conditions

In all the computations presented so far consideration has been given to 2D conditions, so that the deformation of the tunnel and the stress distribution around it (including the extent of the plastic zone, where appropriate) are assumed to occur independently of the tunnel face. However, if the attention is posed on the excavation and support methods currently adopted, it is clear that by doing so important features of tunnel behaviour are being neglected. As demonstrated in the following, this appears to be a simplification of the real problem, particularly when squeezing rock conditions are to be dealt with.

- **Stress path at the tunnel perimeter**

Therefore, it is of interest to pay attention to the pattern of stress and deformation in the rock mass surrounding the face of an advancing circular tunnel (Barla M., 2000). An effective way to do this is to use the stress path representation, as proposed by Lambe (1967) for a number of applications in Geotechnical Engineering. For the purpose of this presentation it is advisable to consider the 8 m diameter tunnel of paragraph 4.2, for the same rock mass and overburden conditions previously analysed.

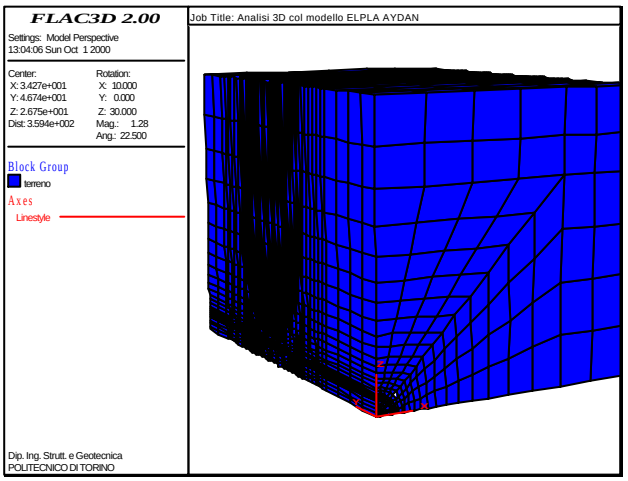

Figure 48: Fully three-dimensional finite difference model

As shown in Figures 48 and 49, a fully three-dimensional finite difference model was created by using the FLAC 3D code (Itasca, 1996) with the purpose to simulate the excavation of a circular tunnel advancing through a weak rock mass subjected to equal stresses in all directions. Let the tunnel be unsupported, i.e. no stabilization measures or linings be installed. As for the two-dimensional case, the stress-strain models (1) and (2) in Figure 32 are considered in con-

junction with the Aydan model (Figure 5). For purpose of comparison, the corresponding results for a linearly elastic rock mass are obtained.

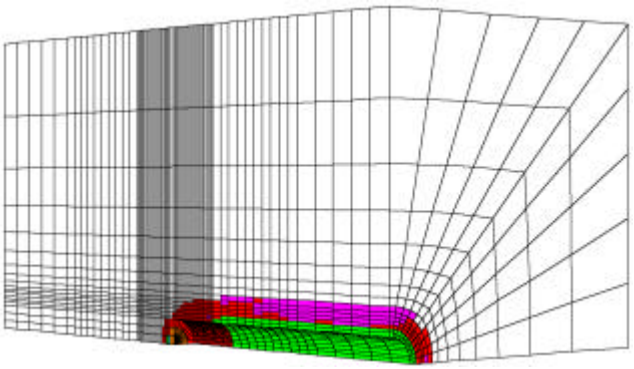

Figure 49: Fully three-dimensional finite difference model. Also shown is the plastic zone around the tunnel. The rock mass behaves according to the Aydan stress-strain law

With reference to either two dimensional or three dimensional analyses the stress path is plotted in the (s, t) plane as follows:

s = mean normal stress = $\frac{\sigma_v + \sigma_h}{2}$

t = deviatoric stress = $\frac{\sigma_v - \sigma_h}{2}$

with:

σ_v = vertical stress;

σ_h = horizontal stress.

The attention is posed on a representative cross section along the tunnel axis in both two and three dimensional conditions; also considered is the stress path at the tunnel face, with the excavation gradually taking place.

Concurrent with excavation (i.e. by allowing a gradual stress relaxation to take place at the tunnel perimeter in a 2D model), the stress path at the crown/invert (C/I) and sidewalls (S), shows the deviatoric stress t to increase, as the normal stress s remains constant, as shown by the vertical dashed line (*Flac*) plotted in Figure 50 for both C, I and S, where the rock mass is assumed to follow a linearly elastic, isotropic stress-strain law.

The stress path is significantly different if a 3D model is considered i.e. the influence of the advancing face of the tunnel is simulated. In these conditions, as shown by the continuous line in Figure 50 (*Flac3D*), the mean normal stress s at the sidewall initially increases, to decrease as soon as the face overpasses the section of interest. An increase of s again occurs as the excavation is completed.

It is obvious to observe that at the crown/invert the same trend of behavior takes place, as for the sidewalls, however with opposite *t*.

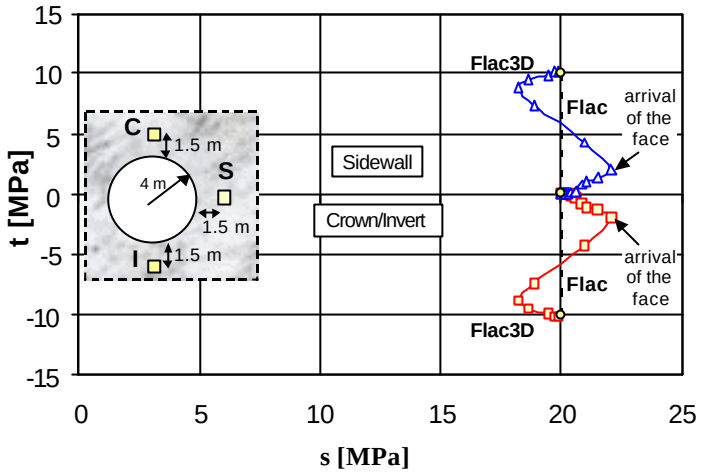

Figure 50: Stress path at point C (crown), I (invert) and S (sidewall) around the tunnel. The rock mass is linearly elastic

This trend of behavior is emphasized even further if one examines the stress path at the tunnel face as the excavation takes place. Figure 51 illustrates it once again in the (*s*, *t*) plane with reference to the elastic perfectly plastic stress-strain law for the rock mass. It is observed that the mean normal stress decreases as the deviatoric stress increases. With the onset of the plastic zone in the cross section of interest, a sudden change occurs in the stress path, as the tunnel face approaches and reaches the cross section of interest.

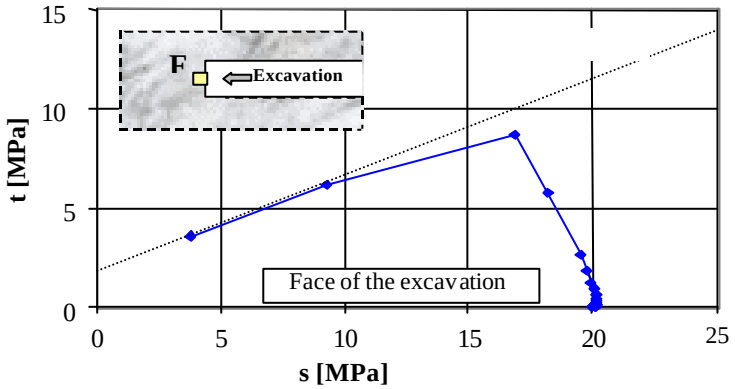

Figure 51: Stress path at point F (face of the excavation). The rock mass is linearly elastic perfectly plastic

Figure 50 shows that, as long as the rock mass in the cross section of interest remains in the elastic state, the stress path computed on the basis of *FLAC3D* gives an increase in the mean normal stress, which is accompanied by a change in the deviatoric stress (positive at the sidewalls and negative at the crown/invert). As the face of the tunnel reaches the same cross section of interest and overpasses it, the mean normal stress decreases, with the deviatoric stress holding approximately constant up to failure.

If consideration is given to the rock mass squeezing behavior by using either the elastic perfectly plastic or the Aydan stress-strain law, the stress path around the tunnel computed by *FLAC3D* changes significantly as shown in Figure 52, being influenced by the advancing tunnel face and the plastic zone which grows and moves with it (Figure 49). On the contrary, the stress path resulting, in two dimensional conditions, from the *FLAC* code (dashed line in Figure 52), shows a decrease in the mean normal stress as the deviatoric stress approaches the failure condition for both the sidewall and the crown/invert.

The stress path for the two models of behaviour (elastic perfectly plastic and Aydan stress-strain laws) shows in both cases a similar trend of behavior, with the Aydan stress-strain law allowing for a greater decrease in the normal stress. Actually, in no case the final state of stress at the sidewalls and at the crown/invert reaches the residual failure value, so that the level of mobilized strain is such as to keep the stress state along the elastic perfectly plastic branch of the Aydan stress-strain law.

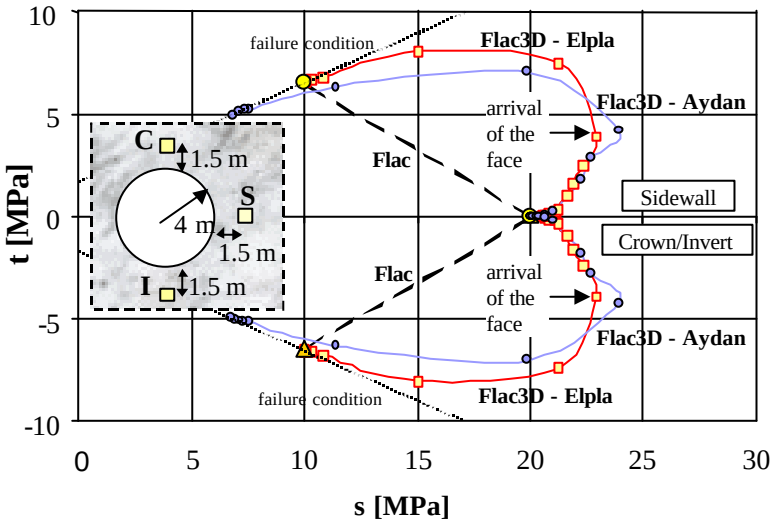

Figure 52: Stress path at point C (crown), I (invert) and S (sidewall) around the tunnel. The rock mass is linearly elastic perfectly plastic (Elpla) or obeys to the Aydan stress-strain law

- **Plastic zone and induced deformation**

Figure 49 shows the plastic zone surrounding the tunnel and the face (for simplicity only the results obtained with the Aydan model are plotted). It is noted that the plastic zone moves in the direction of the tunnel advance as the excavation takes place. Concurrent with the growth of the plastic zone, radial displacements occur behind and ahead of the tunnel face; at the same time inward displacements are induced at the face as illustrated in Figure 53.

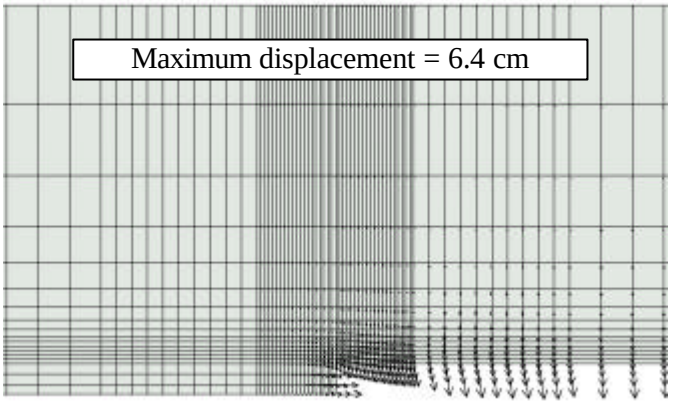

Figure 53: Displacement distribution around the tunnel. The rock mass is behaving according to the Aydan stress-strain law. Longitudinal cross section

The maximum tunnel displacement is given in Table 7, where also shown is the extent of the plastic zone; for the three dimensional case the radial displacement is that computed about two tunnel diameters behind the face, where it reaches the final value. In addition to the elastic perfectly plastic and Aydan models, also reported are the results for the stress-strain law with brittle behaviour.

It is noted that, for the overburden condition under consideration, the first two models of behaviour give nearly the same results for both the extent of the plastic zone and the radial displacements, with the 3D values being slightly higher than those obtained in 2D conditions. In all cases the elasto-plastic stress-strain law with brittle behaviour shows a tendency to overestimate significantly both the displacements and the extent of the plastic zone.

Table 7: Results of 2D and 3D analyses

analysis	3D		2D	
	R_{pl} (m)	u_{max} (cm)	R_{pl} (m)	u_{max} (cm)
perfectly plastic	7.4	5.6	7.0	3.8
brittle	18.4	53.9	18.7	41.0
Aydan	8.2	6.4	7.7	4.7

If a close attention is devoted to the pattern of tunnel deformation in the rock mass ahead and behind the tunnel face, the radial displacements appear to be distributed as shown in Figure 54. It is noted that the deformation in the rock mass starts about one half a diameter ahead of the advancing face (i.e. 12 m ahead) and reaches its maximum value about two diameters behind the face (i.e. 16 m behind). The radial displacement at the face ranges from 0.15 to 0.25 the final displacement depending on the stress-strain model considered.

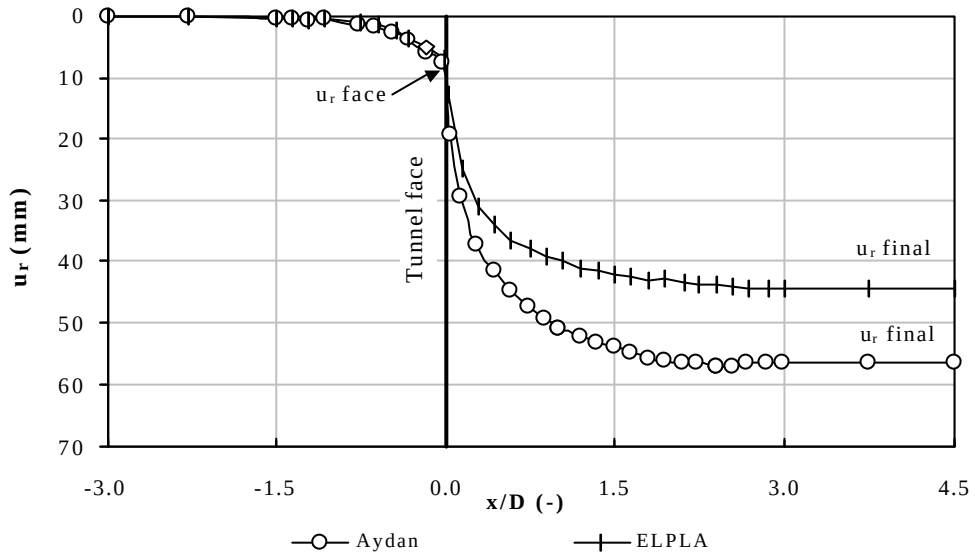

Figure 54: Radial displacement distribution around the tunnel. The rock mass is behaving according to either the elastic perfectly plastic (ELPLA) or the Aydan stress-ratio law. Longitudinal cross section

Another point of interest with reference to the deformation of the rock mass is the horizontal displacement distribution ahead of the face which is illustrated in Figure 55. This plot is intended to account for the horizontal displacement induced in the rock core as the tunnel advances toward the section of interest. It is noted that the greatest horizontal displacements occur for the elasto-plastic brittle model as the influence due to excavation moves behind the face to a distance about one half to two tunnel diameters.

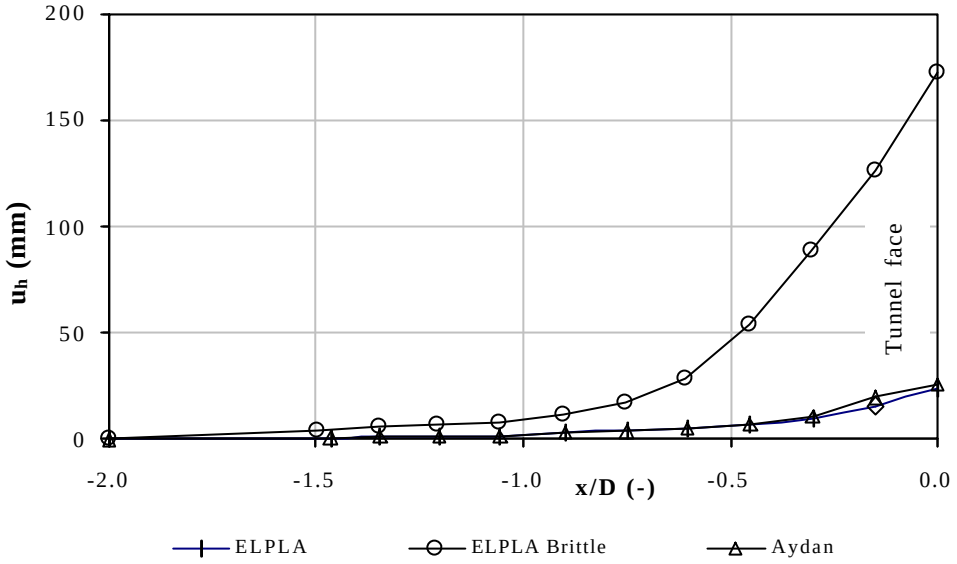

Figure 55: Horizontal displacement distribution ahead of the tunnel face. The three models of behaviour are considered for the rock mass. Longitudinal cross section

6. Observation and monitoring during excavation

As described above, an increased ability to carry out design analyses of tunnels by using closed-form solutions and numerical methods, to a high degree of complexity if required, is available. However, it is also apparent that in squeezing rock conditions these analyses can gain in value if associated to observation and monitoring, which should become an integral part of the construction scheme. With the additional information thus obtained, the design can be adjusted accordingly.

Observation and monitoring during excavation are intended to fulfill the following main objectives:

- to evaluate the stability of the tunnel and of the face
- to extrapolate observed behaviour to sections yet to be excavated
- to provide factual documentation of tunnel performance as a function of rock conditions and construction methods adopted
- to provide valuable data for interpretation and back analysis, in order to clarify design assumptions and improve models of behaviour for rock mass and rock-structure interaction.

6.1 Concepts

According to Peck (1972), observation includes instrumentation. Thus, it is generally agreed to conceive an observational program for tunnelling by comprising: 1) primary observation and 2) instrumented observation (O'Rourke, 1984).

Primary observations comprise: rock mass characteristics including rock mass classification; characters of discontinuities, faults and shear zones (it is recommended to adopt qualitative and quantitative descriptions as suggested by ISRM); water inflow; amount of overbreak; type and quantity of support measures; etc. In squeezing rock conditions these observations may become extremely valuable for a first sight rock identification, considering that in the most difficult cases it may be impossible to obtain samples for testing.

Instrumented observations comprise instrumented tunnel sections for measuring displacements, deformations, pore pressure, … around the tunnel and ahead of the advancing tunnel face, including the structural components used for support. In all cases this implies accurate installation, monitoring and maintenance so that the data obtained are made available in a timely fashion.

It is noted that observation and monitoring in both conventional and TBM tunnelling are characterized by a different degree of constraint depending on the excavation/support options adopted and the rock conditions encountered during face advance. In general, with conventional methods a reasonable time is available for observation, although in cases the need for early support installation may be the cause of difficulty. In TBM excavated tunnels, the face is not accessible and the rock mass just behind the TBM head may be difficult to observe even with open TBM's, when the rock conditions are difficult and need early installation of support.

Observation and monitoring inevitably will interfere with construction activities on site. It is therefore important to establish timely and correctly a close relationship between the contractor and the personnel who will install the instrumentation and will take care of subsequent readings. The contractor may be willing to accept the likely constraints due to installation of instrumentation if he is made part of the information obtained and this is provided in a timely fashion. It is noted that far too often the results of observation and monitoring are not being used in a way to provide the information at precisely the time it is needed.

It is important to note that not very often the results of instrumentation are such as to stimulate modifications in design and construction procedures. In cases, the contractor may be not willing to accept the results of monitoring if this implies a change in the stabilization measures to be adopted, with reduction in ex-

penses. Likewise, the owner may be in the position not to accept the modifications in design and construction procedures if this implies a cost increase. Therefore, it is extremely important to state, right from the beginning of the observational program, that monitoring is going to be used for such a purpose and that all the contractual options for making this effective have been taken into account.

6.2 Summary of instrumentation

The instrumentation within the tunnel will include ([6]):

- convergence measuring points between which accurate measurements are made with tape extensometers (accuracy of measurements: ±0.5 mm), and/or geodetic measurements from a remote theodolite station (accuracy of measurements: ±1.0 mm) without disruption to normal operations (relative movement is measured with the tape extensometers while absolute movement with geodetic measurements);
- extensometers measurements for determining relative displacements between points in a borehole in the direction of the borehole axis (accuracy of measurements: ±0.5 mm); these measurements are generally performed by multiple point borehole extensometers installed in boreholes oriented in a desired direction around the tunnel;
- sliding deformeter measurements for determining relative displacements between points in a borehole drilled in a direction parallel to the tunnel axis, starting from the face (accuracy of measurements: ±0.02 mm/m); measurements are carried out by means of a portable measuring probe and are possible concurrently with face advance;
- strain measurements in the support elements (shotcrete and concrete linings, steel ribs, dowels or anchors, etc.) by means of strain gages attached to steel members or imbedded within shotcrete/concrete (accuracy of measurements: ±0.1%); also used are load cells, concrete stress cells, hydraulic flat jacks;
- pore water pressure measurements by means of piezometer cells installed in boreholes; pneumatic, vibrating wire and electrical resistance piezometers can be used; whichever is adopted, it is important to know the conditions of installation and the ground in which the piezometers cell has been placed.

For purpose of illustration typical monitoring stations are shown in Figures 56 and 57. Figure 56 gives a tunnel excavated by the heading and benching down excavation method where both convergence measuring points and multiple

([6]) Only instrumentation installed within the tunnel is considered in the following. It is reminded that when tunnels are driven at a shallow depth, e. g. in urban areas, additional instrumentation will be needed, which is installed at the surface and in boreholes from the surface.

point extensometers are installed. With the intention to draw the attention on the displacement measurement at the tunnel face and in the rock mass ahead during excavation, Figure 57 illustrates a typical section with measuring points on the face and within the rock mass ahead by means of a sliding micrometer.

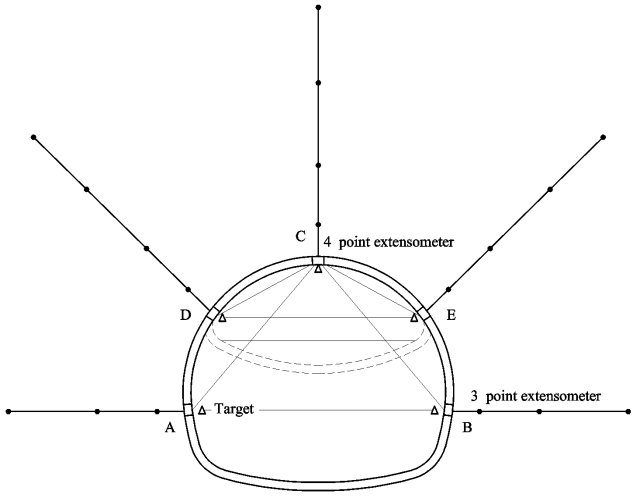

Figure 56: Typical monitoring station with convergence measuring points and multiple point extensometers

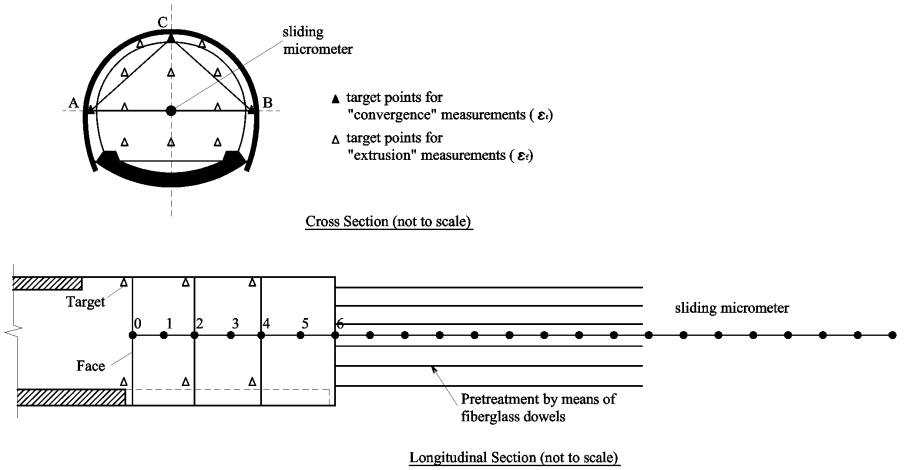

Figure 57: Typical monitoring station with target points on the face and sliding micrometer ahead of the face (not to scale)

6.3 Observation and monitoring of a test tunnel

As suggested for swelling rocks (ISRM, 1994), also for squeezing rock conditions it is advisable, whenever possible, to use observation and monitoring of a test tunnel (access tunnel, side adit, pilot tunnel, etc.). The test tunnel is to be excavated well in advance of the actual tunnels in order to obtain the following information:

- identification and quantification of the squeezing behaviour, mainly the ratio of rock mass strength to in situ stress as an indication of the stability conditions of the rock mass surrounding the advancing tunnel;
- in situ observation and monitoring of tunnel convergences and deformations around the tunnel, including the tunnel face and support/pre-support measures:
- comparison of predicted and observed performance in order to improve the computational approach used and to obtain the rock mass parameters for final design;
- analyse the tunnel response during face advance, by comparing different support measures and excavation sequences, in the attempt to experience passive, active and intermediate design concepts.

Special care need be devoted, during performance monitoring of the test tunnel, to the evaluation of the time dependent behaviour of the rock mass. This is a rather difficult task, especially if one is to determine the rock mass creep parameters to be used in the constitutive laws which will be applied for design purposes. Successful examples of application of this type have been reported by Sulem et al. (1987).

6.4 Convergence measurements interpretation

A common approach in observation and monitoring is the use of convergence measurements. As described by Sulem (1994), one need to be careful as convergence of a tunnel is due to:

(a) the effect of the face advance
(b) the time-dependent behaviour of the rock mass.

The time-dependent face advance has to be recognized and separated from the time-dependent rheological behaviour of the rock mass. This is possible by plotting the convergence C versus the distance of the instrumented section to the face of excavation x and versus time t (see Figure 58). While the face is close to the observation section, the dominant parameter is the distance to the face and, on the other hand, when the face is far ahead its influence vanishes and the tunnel response is controlled by the rheological behaviour of the rock mass.

As described by Sulem (1994), a law used to differentiate the face advance effect from the rock mass time-dependent behaviour is written as follows:

$$C(x,t) = C_{\infty} \cdot f(x) \cdot [1 + mg(t)] \cdot \tag{47}$$

where:

$$f(x) = 1 - \left(\frac{X}{x + X} \right)^2 \cdot \tag{48}$$

$$g(t) = 1 - \left(\frac{T}{t + T} \right)^n \cdot \tag{49}$$

for:

X	=	distance related to the distance of influence of the face;
T	=	characteristic time related to the time-dependent behaviour of the rock mass;
C_{∞}	=	"instantaneous convergence" obtained in the case of an infinite rate of advance (no time dependent effect);
C_{∞} $(1+m)$	=	final convergence;
n	=	exponent greater than zero; in cases of interest (Sulem et al.; 1987a) n = 0.3.

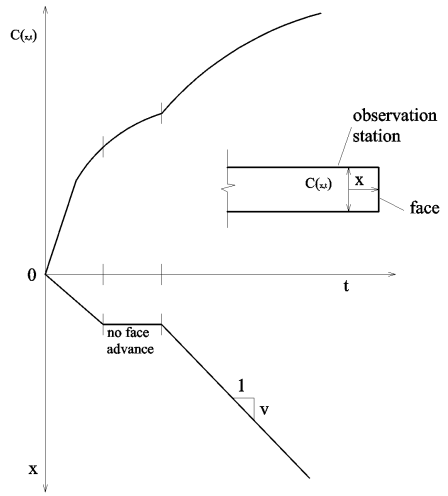

Figure 58: Typical convergence measurement *C (x, t)* versus time *t* and progress of excavation *x*

It is shown that when $x / X \leq 3$, i.e. when the face is not far from the observation station, and $t / T \leq 10$, i.e. when the time of convergence measurement in the observation station is relatively short, the convergence $C(x, t)$ is dependent upon the influence of the advancing face. Viceversa, as the face moves far way from the same station ($x / X > 5$), the convergence is dependent upon the rheological behaviour of the rock mass. It seems reasonable, near to the tunnel face, to analyse the convergence measurements independent of time; when the face is sufficiently far, then most of the attention should be paid to the time dependent behaviour of the rock mass.

Another point of interest is that the distance of influence of the face (i.e. the parameter X) can be shown to depend upon the extent of the plastic zone around the tunnel. In the case of an unlined circular tunnel driven through an elasto-plastic rock mass (the stress-strain model is ideally plastic according to the Mohr-Coulomb yield criterion) in a hydrostatic stress field, the convergence $C(x)$ is (Panet and Guenot, 1982):

$$C(x) = C_{\infty}\left[f(x)\right] = C_{\infty}\left[1 - \left(\frac{0.84 R_{pl}}{x + 0.84 R_{pl}}\right)^2\right] \qquad (61)$$

where:
R_{pl} = radius of the plastic zone for $p_i = 0$.
The convergence law as described above can be used effectively in tunnel practice in squeezing rock conditions as shown by Panet (1996). Once an excavation/construction sequence is being applied in a continuous, systematic fashion and convergence measurements are carried out as a function of the distance x and time t (Figure 58), analytical and numerical calculations by curve fitting procedures allow one to do the following:

- to determine parameters X, T, m, n for a set of cross sections where convergence measurements are available by using equations 58, 59 and 60;
- to evaluate parameter C_{∞} for any new excavated section by curve fitting of the first convergence measurements and eventually to update X, T, m, n;
- to assess the radius of the plastic zone by means of equation 61;
- to anticipate the final tunnel convergence $C_{\infty}(1 + m)$.

6.5 Deformation ahead of the tunnel face

It has already been observed that the understanding of the tunnel deformation e_t (this can be carried out by convergence and extensometer measurements) is as important as to know the face deformation e_f (which is obtained by means of extrusion measurements). In connection with the full face excavation method in

particular, both the stability of the face and the stiffness of the core ahead can be assessed during face advance. This aspect of the problem which is very relevant for tunnelling under squeezing conditions is discussed in the following.

It is noted that a theoretical framework for interpretation of the deformations which occur at the face and in the rock mass ahead is not yet available. As discussed above some preliminary guidelines have been given by Hoek (2000) to estimate both e_t and e_f . Recently, Wong et al. (2000) developed an analytical solution on the general behaviour of the tunnel face, reinforced with fiberglass dowels, by using the homogenization method and the assumption of hydrostatic state of stress. Either elastic or elasto-plastic stress-strain laws can be considered.

The results of monitoring during face advance (the instrumentation used in such a case is shown in Figure 73 and consists of a number of convergence stations, a slide micrometer installed along the tunnel axis, and a number of target points linked to the face) give the horizontal displacements within the rock mass as the reinforced core is gradually being removed, associated with the convergences which are measured concurrently. A typical plot is shown in Figure 59 as reported by Lunardi (1995) for the San Vitale tunnel in Italy.

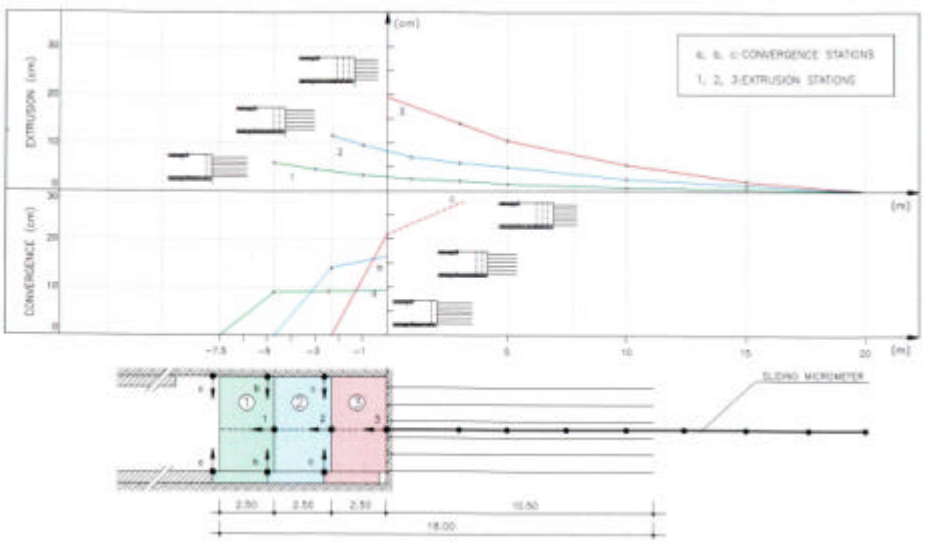

Figure 59: Caserta-Foggia railway line - San Vitale tunnel. Extrusion and convergence measurements during face advance (Lunardi, 1995)

7. A case example: the Pinglin tunnel (Taiwan)

The Pinglin tunnel crosses the Central Mountain Range rock mass; it is located at an average depth of 400 m (the maximum expected depth is 720 m approximately) and comprises two parallel tunnels (called “East Bound” and “West Bound”), with 11.7 m diameter, excavated with a distance center to center of 60 m, which reduces to 42 m approximately in the first 800 m from the portals (Figure 60). The excavation of the two tunnels has been preceded with the excavation of a 5.2 m pilot tunnel, located between the two main tunnels ([7]).

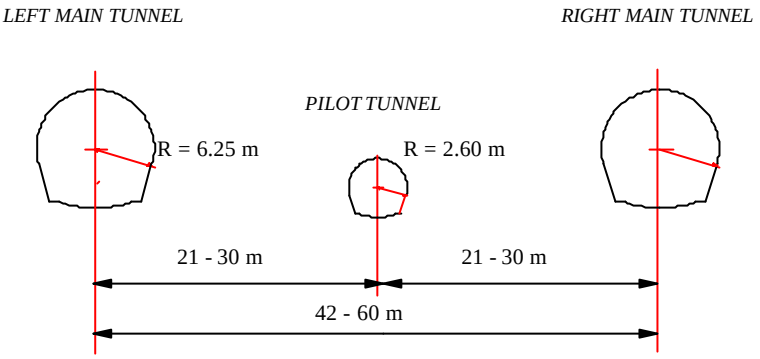

Figure 60: Cross section of the Pinglin tunnel

- **A brief outline of the construction process and monitoring**

The construction process of the Pinglin tunnel foresees mechanized excavation with a TBM along almost the total length, except for the short length near the portals where excavation was to take place by the conventional Drill and Blast method. As very difficult rock mass conditions were encountered at the East portals, the conventional method was used over a greater length than initially expected, prior to reaching a fault zone (Chingyin Fault), which was foreseen 800 m ahead from the portals.

The excavation of the pilot tunnel was initiated in July 1991; in one year the first 520 m were excavated by Drill and Blast, to follow up with mechanized excavation by TBM in July 1992. The new execution process was characterized by a number of problems: the TBM was blocked a few times and the stability conditions became particularly severe when crossing the Chingyin Fault. Following this, a 700 m additional length of the pilot tunnel were excavated, before

([7]) The experimental results used in the present paper were made available during a consulting job carried out in 1995 on behalf of Spie-Batignolles, Paris.

stopping the face advance, following the ninth TBM blockage, 1500 m ahead of the East portal.

The excavation of the two main tunnels was undertaken one year after the pilot tunnel commencement, on July 1993. In both tunnels excavation took place initially by the conventional method. The face advance revealed to be very difficult due to a number of stability problems which were encountered, prior to reaching the fault zone.

Along the main tunnels, two monitoring sections were utilized as follows (Figure 61):

- the first one, with five convergence measuring points: one at the crown, the other ones at the boundary of the excavation placed according to horizontal lines, in order to monitor the crown and bench section excavations; convergence measurements were performed along the lines H1, H2, Dl, D2, D3, D4; in addition, the settlement of the crown was monitored by means of topographic measurements
- the second one, which comprises five multi-point extensometers in addition to the convergence measuring points as above (the extensometer points are at 2 m, 4 m and 6 or 9 m distance from the tunnel contour).

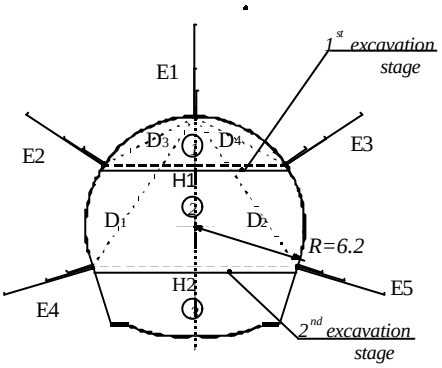

Figure 61: Monitoring system of main tunnels; the continuous lines show the excavation sequence

The main monitoring stations with both multiple point borehole extensometers and convergence measuring points were installed every 200 m along the tunnel axis, whereas the convergence stations were placed every 50 m. Along the first 800 m approximately from the entrance, each tunnel was monitored with three main stations whereas only 13 convergence stations were installed. The attention in the following will be devoted to the first two main stations installed along the left main tunnel, at chainage PK39+972 and PK39+694 (Figure 62).

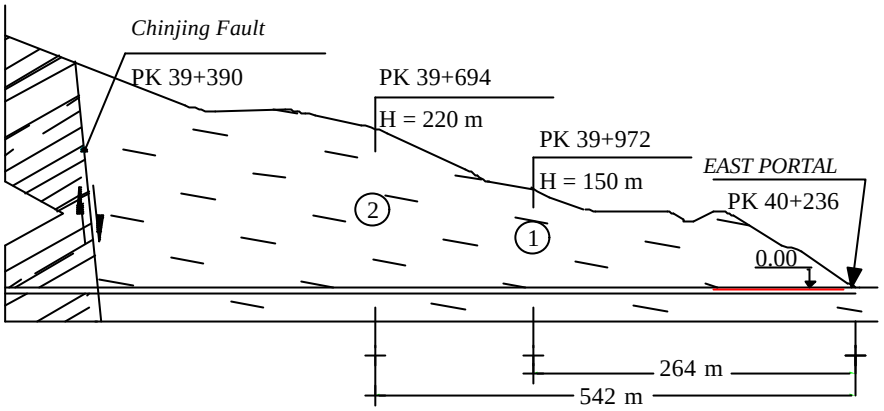

Figure 62: Monitoring sections in the left main tunnel

- **Geotechnical characterization**

The rock mass encountered along the tunnel is argillite with the following characteristics:

- unit weight: 25 kN/m^3
- uniaxial compressive strength of the rock material: 30÷40 MPa
- RMR quality index: 10÷40.

No data were available from in situ tests. Therefore, the rock mass strength and deformability properties were assessed on the basis of well known empirical correlations (Serafim and Perreira, 1983; Hoek and Brown, 1980), by assuming the m_i (coefficient in the Hoek-Brown criterion) value to be equal to 5.

Given that the interest here is to apply the proposed approach as previously shown, it was necessary to assess the strength parameters c and ϕ. This was done by a linearization of the Hoek-Brown criterion for a σ_3 value equal to the isotropic stress p_0. The deformability and strength parameters adopted are given in Table 8. The Poisson's ratio was taken equal to 0.35.

Table 8: Geotechnical properties for the rock mass in the left main tunnel

section (chainage)	H (m)	p_0 (MPa)	RMR	E (GPa)	f_p (°)	c_p (MPa)	f_r (°)	c_r (MPa)
1 (PK 39+972)	150	3.75	18	1.58	17.4	1.18	5.17	0.34
2 (PK 39+694)	200	5.5	15	1.33	13.6	1.33	3.63	0.35

- **Rock mass behaviour**

On the basis of the available data, it was possible to notice that the tunnel exhibits, in the two sections of interest, a squeezing behaviour according to the

empirical criteria due to Singh et al. (1992) and Aydan et al. (1993): for each chainage and the corresponding depth H, the critical value of Q was derived by the following formula (Singh et al., 1992):

$$H = 350 \cdot \sqrt[3]{Q} \cdot \tag{50}$$

Then, by using the empirical correlation formula reported by Bieniawski (1989), the corresponding RMR value was obtained. It is relevant to remark that these values compare well with the "real" ones, as assessed during tunnel excavation: this comparison leads one to conclude that in both the tunnel sections under study squeezing conditions occur according to Singh. The numerical values derived are summarized in Table 9 and illustrated on the *Q-H* plot given in Figure 63.

Table 9: Squeezing behaviour according to Singh et al. (1992), for sections 1 (PK 39+972) and 2 (PK 39+694)

section (chainage)	H (m) (depth)	Q_{singh}	RMR_{Singh}	RMR
PK 39+972	150	0.078	21	18
PK 39+694	220	0.248	31.5	15

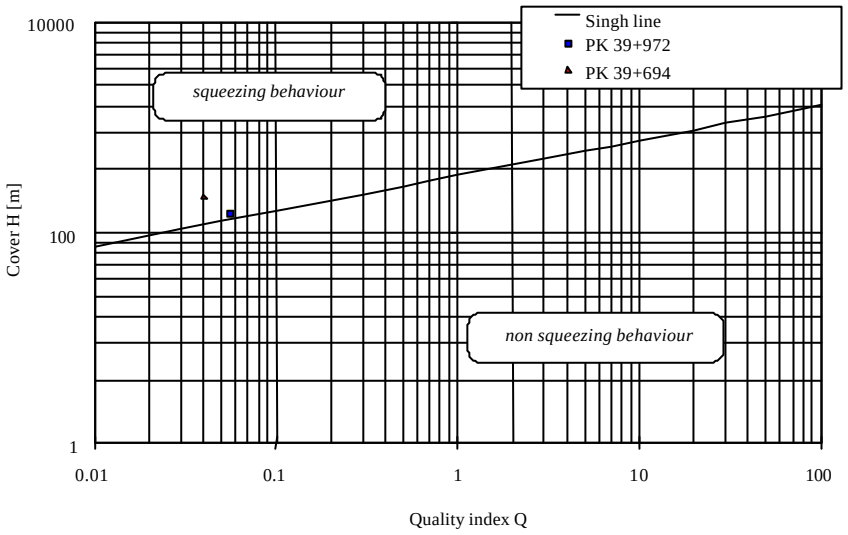

Figure 63: Squeezing behaviour in cross sections 1 (PK 39+972) and 2 (PK 39+694) according to Singh et al. (1992) criterion

In a similar way, also applied was the criterion given by Aydan et al. (1993), who state that squeezing conditions occur when:

$$\alpha = \frac{\sigma_{cm}}{\gamma \cdot H} < 2 \tag{51}$$

where σ_{cm} is taken as the rock mass uniaxial compressive strength, γ is the unit weight and H is the tunnel depth.

As already pointed out, the rock material uniaxial compressive strength is σ_c = 35÷40 MPa. Therefore, by using the Hoek-Brown criterion, the corresponding rock mass strength is given by:

$$\sigma_{cm} = \sqrt{s} \cdot \sigma_c \tag{52}$$

where s is easily assessed on the basis of the RMR index (Hoek and Brown, 1998).

The results obtained are summarized in Table 10 for the two tunnel cross sections of interest; it is noted that in both cases the α values are significantly smaller than 2 and that the left main tunnel is, in the length under consideration, under squeezing conditions.

Table 10: Squeezing behaviour in cross sections 1 (PK 39+972) and 2 (PK 39+694) according to Aydan (1993) criterion

section (chainage)	H (m) (depth)	s	σ_{cm} (MPa)	α
PK 39+972	150	0.0061	2.7	0.72
PK 39+694	220	0.0075	3.0	0.655

- **Tunnel section at chainage PK 39+976**

The considerations below have been derived by referring to the convergence data available for the tunnel section at chainage PK 39+976, i.e. 260 m approximately from the entrance, under a depth of cover equal to 150 m. The rock mass conditions were assessed to be "poor" (class V); the excavation sequences were as follows: top heading, first and second benching down, invert excavation. The primary lining consists of mesh reinforced shotcrete (20 cm thick), steel sets (HE 100x100 mm) and rock bolts (length 6 m).

The monitored displacements at the crown (V1) and the horizontal convergence (HI and H2) are plotted versus time in Figure 64. It is possible to notice that the maximum displacement (V1) is at the crown and is equal to 215 mm. This gives a u_{rad} / a ratio equal to 3.44%. Accordingly, for the H2 convergence equal to 163 mm the corresponding value is 1.3%.

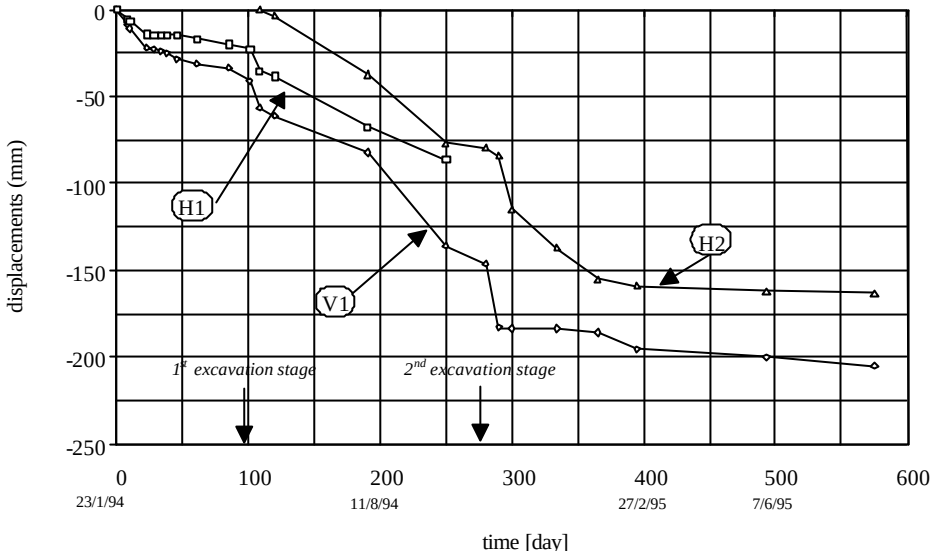

Figure 64: Convergences H1 e H2 and crown displacement (V1) measured in the cross section 1 at chainage PK 39+972

It is of interest to note that, based on the convergence response as shown in Figure 64, the opening of the crown heading does not result in a stable condition: e.g. along the H1 length a convergence rate of 5 mm/month occurs; with the first benching down, this convergence rate attains even greater values up to 13 mm/month; only with the second benching down (after six months from the first benching down) and invert excavation, followed by immediate ring closure with a reinforced concrete invert, the convergence rate becomes smaller (2 mm/month approximately).

The significant convergence rate values, as experienced by the tunnel cross sections between the first and the second benching down for a significant time period, let one think that the rock mass exhibits a viscous-plastic behaviour. This is well confirmed by the convergence versus time measured along the 112 m length following the second benching down: in approximately three months the convergence doubles its value. Also, the measurements along H1 were no longer possible after 8 months as a consequence of damage of the measuring pins.

As an additional point of interest, it is relevant to analyze the convergence measured in the pilot tunnel, which was excavated ahead of the two main tunnels, thus allowing one to understand the rock mass response due to excavation and to assess the following:

- the influence on the pilot tunnel stability as due to the face advance of both the main tunnels
- the mutual interaction between the pilot tunnel and the main tunnels.

Figure 65 shows the convergence for the pilot tunnel in a cross section at chainage 350 m from the entrance; it is possible to note that the convergence which occurs as a consequence of the pilot tunnel excavation has a tendency to decrease when the face is 15 m ahead of the monitoring station, then to increase very slowly, at a rate of only 0.8 mm/month: in these conditions the tunnel cross section is therefore stable with a very limited time-dependent behaviour.

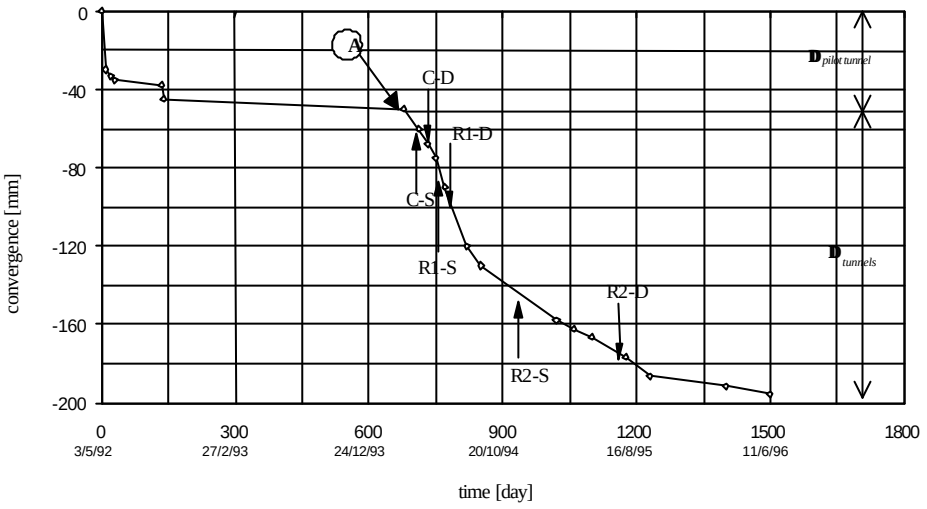

Figure 65: Convergences in the pilot tunnel at cross section 40+328 due to excavation in the main tunnels
C-D = crown 1st excavation stage in the right main tunnel
R1-D= 2nd excavation stage in the right main tunnel
R2-D= 3rd excavation stage in the right main tunnel
C-S = crown 1st excavation stage in the left main tunnel
R1-S = 2nd excavation stage in the left main tunnel
R2-S = 3rd excavation stage in the left main tunnel

The deformational response appears to peak up very significantly with the approaching of the face excavation of the two main tunnels. The rate of convergence shows an increase when the top headings of the main tunnels are 50 m approximately behind the monitoring station in the pilot tunnel (point A in Figure 65), then to attain significantly high values with the main tunnels approaching.

It is possible to derive the following remarks:

- given that the pilot tunnel has been excavated 500 m ahead of both the headings of the main tunnels, the convergence $D_{pilot\ tunnel}$ shown in Figure 65 gives the rock mass deformational response due to the pilot tunnel excavation only; a strong increase in convergence follows up due to the influence of the excavation of the main tunnels; this results in a significant change in the state of stress so as to determine large plastic zones with extent so as to reach the pilot tunnel
- the excavation of the pilot tunnel only exhibits a very small time dependent behaviour, which however is negligible with respect to the response observed during the main tunnel excavations; this is to be related to the comparatively small size of the pilot tunnel.

- **Numerical analyses performed**

The main tunnels response to excavation has been analyzed by considering one tunnel only, under the assumption of symmetric conditions with respect to the axis between the two openings. The finite difference method and the FLAC code were utilized according to the following:

- elasto-plastic brittle behaviour
- squeezing behaviour.

The stress-strain model adopted in order to describe the squeezing behaviour is shown in Figure 66. As described in detail by Barla and Borgna (1999), the following three stages of behaviour are considered:

- Linearly elastic stage (OA), which applies up to the stress level s_{1A}, when the ground starts to exhibit a time-dependent behaviour
- Hardening stage (AB), which is intended to represent the terminal locus of creep strain, without resulting into creep failure
- Long-term stage (BC), when a strain softening behaviour is assumed.

As already anticipated, the implementation of this stress-strain model is possible by the finite difference method and the FLAC code, which enables the user to incorporate the desired changes in the available constitutive laws and to define continuous functions of the strength parameters based on the actual stress-strain level. The Mohr-Coulomb plasticity model has been adopted to suit the specific needs of the stress-strain model above.

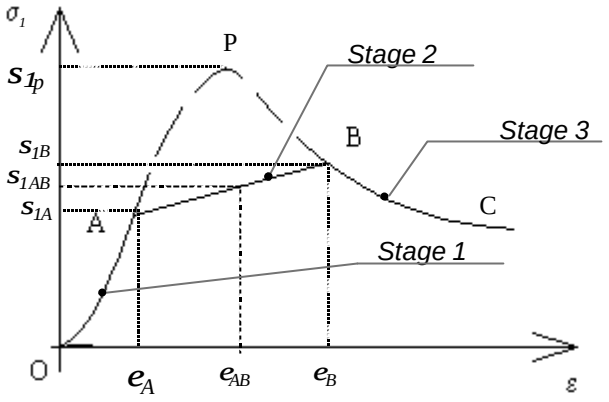

Figure 66: Model adopted for analysis of squeezing behaviour of the Pinglin tunnel

With reference to the convergence measured along the H2 length, a series of sensitivity analyses were carried out by using the model of behaviour in Figure 66 with the s_A / s_p ratio taken as 0.64. The computed value of convergence is equal to 166.4 mm (horizontal displacement 83.2 mm, Figure 67), which compares reasonably well with the measured 163.2 mm. It is noted that the corresponding analysis for the elasto-plastic-brittle model and the set of parameters shown in Table 8 gives a computed convergence of 84.2 mm (horizontal displacement 42.1 mm, Figure 67).

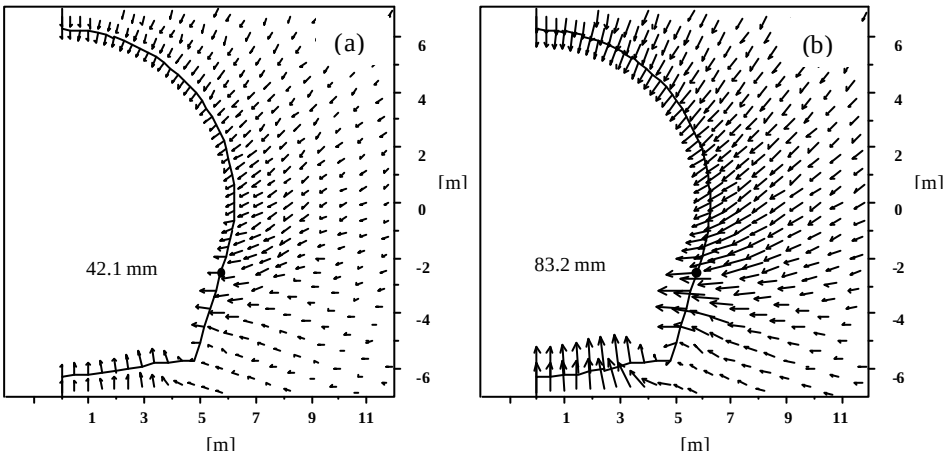

Figure 67: Computed displacements in the tunnel surround: (a) elastic-plastic-brittle model; (b) proposed model

Also of great significance are the results obtained for the plastic zones around the tunnels. Figure 68 shows these zones for the squeezing and the elasto-

plastic-brittle model respectively: it is clear that the first model gives a plastic zone which extends nearly twice as that computed for the second model. This type of behaviour is taken as representative of the expected response of the tunnel in the real conditions.

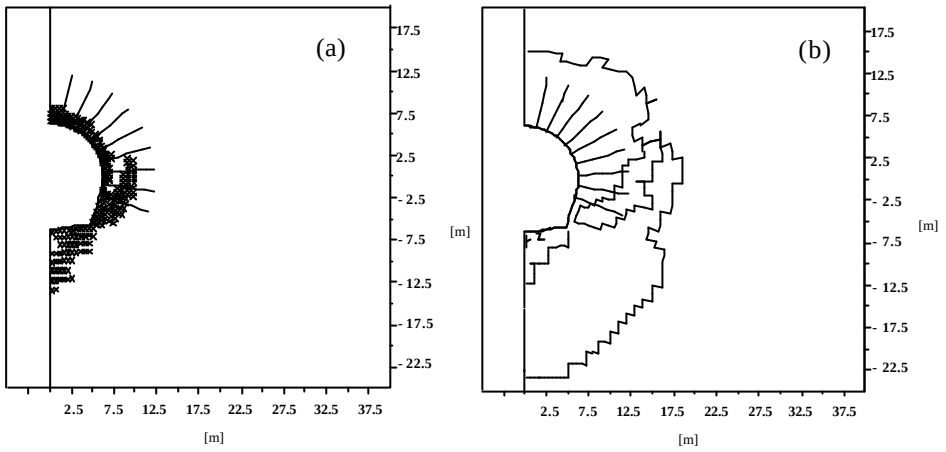

Figure 68: Plastic zone around the tunnel: (a) elastic-plastic-brittle model; (b) proposed model

By paying attention to the convergence experienced by the main tunnels and the pilot tunnel, it is evidenced that when the heading of the main tunnel approaches the preexisting pilot tunnel a significant interaction takes place, with influence on its stability conditions (see Figure 26). This behaviour is linked to the spreading of the plastic conditions within the rock mass between the two tunnels: according to a stress analysis carried out for the pilot tunnel only under the assumption of squeezing behaviour, the extent of the plastic zone, along the line joining the main tunnel centers, is approximately equal to 5 m.

If consideration is also given to the extent of the plastic zone computed around the main tunnel, it is possible to assume that the size of the plastic zones increases up to obtaining a very extended zone of disturbance surrounding the two tunnels. It is relevant to point out that this condition is likely to have taken place in the real case, as well evidenced by the damages occurred in the support of the pilot tunnel. This is not the response obtained if the elasto-plastic brittle behaviour is assumed, unless very low and unreasonable values are given to the strength parameters.

- **Considerations**

The results obtained show that, under squeezing behaviour, the elasto-plastic models fail to reproduce the deformational response which takes place during

tunnel excavation. At the same time, the adoption of more complex models of behaviour is not easy to be proposed in view of the generally poor rock mass conditions which make it difficult to obtain representative samples for testing under time-dependent conditions. Also, the problems met during excavation do not always allow performance monitoring for the same purpose (they would require one to stop face advance for a long time period). Therefore, the characterization of the rock mass rheological properties from in situ monitoring may become very difficult if not impossible.

The use of the stress-strain model shown in Figure 66 allows one to overcome some of these limitations by means of reasonable assumptions for the squeezing behaviour, based on design parameters for deformability and strength, which are possible to be obtained in practice. For the case study of the Pinglin tunnel (Taiwan), the more extended plastic zone obtained with this approach when compared to the elasto-plastic-brittle solution, allows one to explain for the interaction taking place between the main tunnels and the pilot tunnel, concurrent with large convergences around it. These occurred when the heading of the main tunnels approached the monitoring station in the pilot tunnel, causing significant damages of the support.

8. References

[1] Aydan Ö., Akagi T., Kawamoto T. (1993) - *The squeezing potential of rock around tunnels: theory and prediction*. Rock Mechanics and Rock Engineering, 2, pp. l37-163.

[2] Barla G., Pazzagli G., Rabagliati U. Travaglini S. (1986) - *The San Donato Tunnel (Florence)*. Congresso Internazionale su Grandi Opere in Sotterraneo, Firenze, pp. 61-69.

[3] Barla G. (1989) – *Stabilization measures in near surface tunnels in poor ground conditions.* International Congress on Progress and Innovation in Tunnelling, Toronto, pp. 203-211.

[4] Barla G. (1995) – *Squeezing rocks in tunnels*. ISRM News Journal, 3/4, pp. 44-49.

[5] Barla G. and Borgna S. (1999) – *Squeezing behaviour of tunnels: a phenomenological approach.* Gallerie, 58, pp. 39-60.

[6] Barla M. (2000) – *Stress paths around a circular tunnel.* Rivista Italiana di Geotecnica, Italian Geotechnical Journal, 34, 1, pp. 53-58.

[7] Barton N., Lien R. and Lunde I. (1974) – *Engineering classification of rock masses for the design of tunnel supports.* Rock Mechanics, 6, 4, pp. 189-239.

[8] Bernaud D. (1991) – *Tunnels profonds dans les milieux viscoplastiques.* Doctoral Thesis, École National des Ponts et Chaussées, Paris.

[9] Bieniawski Z.T. (1989) – *Engineering rock mass classifications.* John Wiley, Rotterdam.

[10] Brady B.H.G. and Brown E.T. (1985) – *Rock mechanics for underground mining.* Chapman & Hall, London.

[11] Brown E.T., Bray J.W., Ladanyi B. and Hoek E. (1983) – *Characteristic line calculations for rock tunnels*. J. Geotech. Eng. Div. Am. Soc. Civ. Eng., 109, pp. 15-39.

[12] Carranza-Torres C. and Fairhurst C. (1999) – *The elasto-plastic response of underground excavations in rock masses that satisfy the Hoek-Brown failure criterion.* Int.J.Rock Mech. Min.Sci., 36, pp. 777-809.

[13] Cristescu N. (1993) – *Rock rheology.* Comprehensive Rock Engineering, Pergamon Press, J.A. Hudson ed., 1, pp. 523-544.

[14] Gioda G. and Cividini A. (1996) – *Numerical methods for the analysis of tunnel performance in squeezing rocks.* Rock Mechanics and Rock Engineering, 29, 4, pp. 171-193.

[15] Goel R.K., Jethwa J.L. and Paithakan A.G. (19) – *Tunnelling through the young Himalayas – a case history of the Maneri-Uttarkashi power tunnel.* Engrg. Geol., 39, pp. 31-44.

[16] Hoek E. and Brown E.T. (1980) – *Underground excavations in rock.* Instn.Min.Metall., London.

[17] Hoek E., Kaiser P.K. and Bawden W.F. (1995) – *Support of underground excavations in hard rock.* A.A. Balkema, Rotterdam.

[18] Hoek E., Brown E.T. (1997) - *Practical estimates of rock mass strength*. Int. J. Rock Mech. Min. Sci., 34, pp. 1156-1186.

[19] Hoek E. (1998) – *Tunnel support in weak rock.* Sedimentary Rock Engineering, ISRM Regional Symposium, Taipei, O. Chin-Der ed., pp. 281-292.

[20] Hoek E. (1998) – *Reliability of Hoek-Brown estimates of rock mass properties and their impact on design.* Int. J. Rock Mech. Min. Sci., 35, pp. 63-68.

[21] Hoek E., Marinos P. and Benissi M. (1998) – *Applicability of the Geological strength index (GSI) classification for very weak and sheared rock masses. The case of the Athens Schist Formation.* Bulletin of Engineering Geology and the Environment, 57, 2, pp. 151-160.

[22] Hoek E. and Marinos P. (2000) – *Predicting tunnel squeezing problems in weak heterogeneous rock masses.* Tunnels and Tunnelling International, pp. 45-51: part one; pp. 33-36: part two.

[23] Hoek E. (1999a) – *Rock Engineering.* Course note available on website: www.rocscience.com.

[24] Hoek E. (2000) – *Big tunnels in bad rock.* Draft of a paper to be submitted for publication in the ASCE Journal of Geotechnical and Geoenvironmental Engineering, 2000 Terzaghi Lecture, Seattle.

[25] International Society for Rock Mechanics (ISRM) (1994) – *Comments and recommendations on design and analysis procedures for structures in argillaceous swelling rock.* Int. J. Rock Mech. Min. Sci., 31, 5.

[26] ITASCA Inc. (1996) – *FLAC 3D Fast Lagrangian Analysis of Continua.* Version 1.1, User's manual.

[27] ITASCA Inc. (1996) – *UDEC (Universal Distinct Element Code).* Version 3.0, User's manual.

[28] ITASCA Inc. (1998) - *FLAC - Fast Lagrangian Analysis of Continua*. Ver. 3.4, User's manual.

[29] Jethwa J.L., Singh B and Singh B. – (1984) – *Estimation of ultimate rock pressure for tunnel linings under squeezing rock conditions – a new approach.* Design and Performance of Underground Excavations, ISRM Symposium, Cambridge, E.T. Brown and J.A.Hudson eds., pp. 231-238.

[30] Kovari K. (1998) - *Tunnelbau in druckhaftem Gebirge - Tunnelling in squeezing rock*. Tunnel 5, pp. 12-31.

[31] Ladanyi B. (1993) - *Time-dependent response of rock around tunnels*. Comprehensive Rock Engineering, Pergamon Press J.A.Hudson ed., vol. 2, pp. 78-112.

[32] Lambe T.W. (1967) – *The stress path method.* Journal Soil Mechanics Foundation Division, ASCE, pp. 309-331.

[33] Lanino G. (1875) – *Gallerie della traversata dell'Appennino nella linea Foggia-Napoli.* Tip. e Lit. del Giornale del Genio Civile, Roma.

[34] Lunardi P. (1995) – *Progetto e costruzione di gallerie secondo il metodo basato sull'analisi delle deformazioni controllate nelle rocce e nei suoli.* Quarry and Construction, pp. 113-138.

[35] Lunardi P. (2000) – *Design and constructing tunnels – ADECO-RS approach.* Tunnels and Tunnelling International, Special supplement May.

[36] Lunardi P. and Bindi R. (2001) – *The evolution of reinforcement of the advance core using fibre glass elements for short and long term stability of tunnels under difficult stress-strain conditions: design, technologies and operating methods.* Progress in Tunnelling after 2000, AITES-ITA 2001 World Tunnel Congress, 2, pp. 309-322.

[37] Moritz A.B. (1999) – *Ductile support system for tunnels in squeezing rock.* Doctoral Thesis, Department of Civil Engineering, Technical University Graz.

[38] O'Rourke T.D. (1984) – *Guidelines for tunnel lining design.* ASCE.

[39] Panet M. and Guenot A. (1982) – *Analysis of convergence behind the face of a tunnel.* Tunnelling 82, IMM, Brighton, pp. 199-204.

[40] Panet M. (1995) - *Le calcul des tunnels par la méthode convergence-confinement.* Presses de l'Ecole Nationale des Ponts et Chaussées, Paris.

[41] Panet M. (1996) – *Two case histories of tunnels through squeezing rocks.* Rock Mechanics and Rock Engineering, 29, 3, pp. 155-164.

[42] Peck R.B. (1972) – *Observation and instrumentation: some elementary considerations.* Highway Focus, U.S. Dept. of Transportation, Federal Highway Administration, pp.1-7.

[43] Ribacchi R. and Riccioni R. (1977) – *Stato di sforzo e di deformazione intorno ad una galleria circolare.* Gallerie e Grandi Opere Sotterranee, 4, pp. 7-17.

[44] Robbins R.J. (1997) – *Hard rock tunneling machines for squeezing rock conditions: three main concepts.* Tunnels for People, 23rd Assembly of the ITA, Vienna, Golser, Hinkel and Schubert eds., pp. 633-638.

[45] Serafim J.L. and Pereira J.P. (1983) – *Considerations of the geomechanics classification of Bieniawski.* Int. Symp. Eng. Geol.: Underground Constr., LNEC, Lisbon, 1, pp. II.33-II.42.

[46] Schubert W. and Schubert P. (1993) – *Tunnels in squeezing rock: Failure phenomena and counteractions. Assessment and prevention of failure phenomena in rock engineering.* International Symposium, Istanbul, A.C. Pasamehmetoglut, I. Kawamoto, B.N. Whittaker, O. Aydan eds., pp. 479-484.

[47] Schubert P. (1996) – *Dealing with squeezing conditions in Alpine tunnels.* Rock Mechanics and Rock Engineering, 29 (3), pp. 145-153.

[48] Schubert W. (2000) – *TBM excavation of tunnels in squeezing rock.* Lo scavo meccanizzato di gallerie, MIR 2000, Torino, G. Barla ed., pp. 355-364.

[49] Singh B., Jethwa J.L., Dube A.K., Singh B. (1992) - *Correlation between observed support pressure and rock mass quality*. Tunnelling and Underground Space Technology, 7, pp. 59-74.

[50] Sing B. and Goel R.K. (1999) – *Rock mass classification: a practical approach in Civil Engineering.* Elsevier Science Ltd. U.K..

[51] Sulem J., Panet M. and Guenot A. (1987) – *Closure analysis in deep tunnels.* Int.J.Rock Mech. Min. Sci. & Geomech.Abstr., 24, 3, pp. 145-154.

[52] Sulem J., Panet M. and Guenot A. (1987) – *An analytical solution for time-dependent displacements in a circular tunnel.* Int.J.Rock Mech. Min. Sci. & Geomech.Abstr., 24, 3, pp. 155-164.

[53] Sulem J. (1994) – *Analytical methods for the study of tunnel deformation during excavation.* Gallerie in condizioni difficili, MIR '94, Torino, G. Barla ed., pp. 301-317.

[54] Terzaghi K. (1946) – *Rock defects and loads in tunnel supports. Rock tunneling with steel supports.* R.V. Proctor and T.L. White eds., The Commercial Shearing and Stamping Co., Youngstown, Ohio, pp. 17-99.

[55] Voerckel M. (2001) – *Tunnelling with TBM. State of the art and future development.* Progress in Tunnelling after 2000, AITES-ITA 2001 World Tunnel Congress, 2, pp. 493-500.

[56] Wong H.K.K., Subrin D. and Dias D. (2000) – *Extrusion movements of a tunnel head reinforced by finite length bolts–a closed-form solution using homogenization approach.* Int. J. Numer.Anal.Meth.Geomech., 24, pp. 533-565.

APPENDIX 1

1. Definitions of squeezing published by the International Society for Rock Mechanics (ISRM), Barla (1995)

Squeezing of rock is the time dependent large deformation which occurs around the tunnel ([8]) and is essentially associated with creep caused by exceeding a limiting shear stress. Deformation may terminate during construction or continue over a long time period.

- Squeezing can occur in both rock and soil as long as the particular combination of induced stresses and material properties pushes some zones around the tunnel beyond the limiting shear stress at which creep starts.
- The magnitude of the tunnel convergence associated with squeezing, the rate of deformation, and the extent of the yielding zone around the tunnel depend on the geological conditions, the in situ stresses relative to rock mass strength, the groundwater flow and pore pressure, and the rock mass properties.
- Squeezing of rock masses can occur as squeezing of intact rock, as squeezing of infilled rock discontinuities and/or along bedding and foliation surfaces, joints and faults.
- Squeezing is synonymous of overstressing and does not comprise deformations caused by loosening as might occur at the roof or at the walls of tunnels in jointed rock masses. Rock bursting phenomena do not belong to squeezing.
- Time dependent displacements around tunnels, of similar magnitudes as in squeezing rock conditions, may also occur in rocks susceptible to swelling. While swelling always implies volume increase, squeezing does not, except for rocks exhibiting a dilatant behaviour. However, it is recognized that in some cases squeezing may be associated with swelling.
- Squeezing is closely related to the excavation and support techniques and sequences adopted in tunnelling. If the support installation is delayed, the rock mass moves into the tunnel and a stress redistribution takes place around it. Conversely, if the rock deformations are constrained, squeezing will lead to longterm load build-up of the rock support.

([8]) The term "tunnel" is used in the following to describe underground excavations in general, including large caverns.

2. Summary of definitions of squeezing as available in the Rock Mechanics literature

- **Definition according to Terzaghi (1946)**

Terzaghi defines squeezing rock and swelling rock as follows:
- squeezing rock is merely rock which contains a considerable amount of clay. The clay may have been present originally, as in some shales, or it may be an alteration product. The rock may be dominated by the inoffensive members of the Kaolinite group or it may have the vicious properties of the Montmorillonites. Therefore the properties of squeezing rock may vary within as wide a range as those of clay;
- the term swelling rock refers to rocks the squeeze of which is chiefly due to swelling. Swelling rocks are always at least moderately dense, having the consistency of stiff or hard, pre-loaded clays.

Terzaghi also points out that:
- squeezing rock slowly advances into the tunnel without perceptible volume increase. Prerequisite for squeeze is a high percentage of microscopic and submicroscopic particles of micaceous minerals or of clay with a low swelling capacity;
- swelling rock advances into the tunnel chiefly on account of expansion. The capacity to swell seems to be limited to those rocks which contain clay minerals such as montmorillonite, with a high swelling capacity.

- **Definition given by Gioda (1982)**

In a paper describing the analysis of "The non-linear squeezing effects around circular tunnels", the term squeezing is taken to indicate the time dependent deformation produced by the concentration of shear stresses in the zone surrounding the excavation. Both deviatoric and volumetric deformations may be present, the latter associated with possible dilatancy of the geotechnical medium.

On the contrary, swelling refers to a time-dependent volume increase produced by absorption of water in the zone close to the excavation. It is noted that the swelling phenomenon is particularly evident in soils and in rocks containing clay minerals with small particles size (such as Montmorillonite) and in rocks containing Anhydrite. In both cases swelling is caused by the physico-chemical interaction between the solid and liquid phases of two-phase media.

- **Definition given by O'Rourke (1984)**

Squeezing ground is defined as ground that undergoes substantial time-dependent deformation in the vicinity of the tunnel as the result of load intensi-

ties exceeding its strength. This loading is brought about by the redistribution of stresses adjacent to the excavated opening. As a consequence of the squeezing ground, the tunnel supports will experience loads that may increase for weeks or even months to a value several times higher than the initial ones. In some instances, it is advantageous to allow movement of the ground before providing support. By doing so, the stresses in the ground redistribute themselves and the support requirements are diminished. Movements of the ground surface above the tunnel, however, may be increased. The design of a tunnel in squeezing ground requires careful study of factors such as in-situ stresses, degree of weathering and mineralogy of the ground, time and stress-dependent strength and deformation characteristics of the ground, and excavation and support techniques and sequences.

- **Definition given by Jethwa (1986)**

Creation of a tunnel opening disturbs the primitive stress field and the rock mass around the opening is strained under the influence of induced stresses. All points around the tunnel are consequently displaced radially into the opening. A support system tries to contain these radial displacements called the tunnel-wall displacements and gets loaded. The rock loads, thus, depend on the magnitude of the tunnel-wall displacements. In case of competent rock masses, these displacement are elastic in nature and remain generally within 1 per cent of the tunnel radius. These are called time-independent displacements and are associated with low rock loads on the support system. These rock loads stabilize soon after excavation and a final concrete lining in hydroelectric tunnels is normally provided from hydrological considerations only. On the contrary, a soft rock mass fails under high primitive stresses and forms a plastic or broken zone around a tunnel opening. The failed rock mass undergoes plastic deformations which continue for months. This is called squeezing rock condition and the tunnel-wall displacements are predominantly time-dependent under such conditions. The rock loads on the support system continue to increase till the rate of tunnel-wall displacement becomes zero. The radial rock pressure acting on the tunnel lining at this stage is called the ultimate rock pressure. The difference between the ultimate and the short-term values of rock pressure is called the creep pressure. The magnitude of the creep pressure under the squeezing rock conditions is considerably greater than the short-term rock pressure. Tunnel linings should, therefore, be capable of withstanding the ultimate rock pressure.

- **Definition by Kovari (1988)**

Squeezing response of the rock to excavation implies:

- large ground deformations causing reduction of cross section possibly even in the floor;

- deformations go on during a long time period;
- if deformations are hindered, great pressures may arise sometimes due to failure of the tunnel support.

Squeezing behaviour is best understood by assuming yielding rock conditions around the opening. Low rock strength versus high stress is decisive. The rock is stressed to its bearing capacity and fails in yielding manner in contrast to brittle failure. Time effects with creep and/or increasing rock pressure is the consequence.

It is also implied that:
- the continuous large deformations are not the result of swelling. Swelling means increase in volume of the rock due to absorption of water. Rock containing clay minerals such as Illite, Montmorillonite and Corrensite and/or Anhydrite are susceptible of swelling;
- large rock deformations restricted to the roof area or to the walls may occur due to inadequate support in jointed rock. These deformations are caused by loosening and not by yielding due to overstressing;
- rock bursting does not belong to the category of squeezing rock.

- **Definition adopted in India (Singh, 1988)**

Squeezing implies rock mass failure (associated with volumetric expansion) due to overstressing and in tunnels it is associated with movements of the failed rock mass into the opening. It is noted that swelling is associated with certain clays e.g. Montmorillonite, Illite, Chlorite, etc. which swell due to the ingress of moisture. Also, it is emphasized that tunnel closures under squeezing conditions may continue for long periods, sometimes over a year.

- **Definition given by Einstein (1990)**

In a comprehensive paper on 'Design and analysis of underground structures in swelling and squeezing rocks", Professor Einstein notes that both swelling and squeezing cause an inward movement of the tunnel periphery over time. The intensity of the movement rate and the magnitude of the displacements often vary over the tunnel surface depending on the geology, on the original stress state and on the shape of the tunnel.

Swelling is due to volume increase caused by water uptake and often occurs without yielding, while squeezing is essentially associated with creep caused by exceeding a limiting shear stress. Nevertheless, in dilatant materials, squeezing can also be associated with volume increase, while on the other hand, swelling induced stresses and material modifications may cause time dependent yielding.

Swelling and squeezing can occur in both rock and soil. Most occurrences of swelling ground are associated with argillaceous soil or rock; swelling in anhydrite or mixed anhydrite-argillaceous rock is less frequent and may actually cause the most severe problems.

Squeezing, as the preceding description of the phenomenon implies, can occur in any soil or rock as long as the particular combination of induced stresses and material properties pushes some zones around the tunnel beyond the limiting shear stresses at which creep starts.

A careful definition of squeezing rock is also given as follows: Squeezing is time dependent shear displacement of the ground which causes the tunnel periphery to move inward. The squeezing mechanism can consist of anyone or a combination of submechanisms, namely:

- creep (or otherwise expressed viscous behaviour) in the particles of the intact material such as the grains in rock and soil. Creep of individual particles may be due to viscous behaviour of the crystal structure or unstable crack propagation;
- creep along the interfaces between particles of the intact material, and creep along larger scale discontinuities such as bedding and foliation surfaces, joints and faults.

These creep mechanisms involve the three well known components (primary, secondary and tertiary) and typical combinations thereof. Usually, the creep mechanisms underlying squeezing is of visco-plastic nature but, particularly at low stresses, some of the strains may be recoverable i.e. visco-elastic behaviour occurs.

Creep usually occurs at stress levels below the short term shear strength of a material. The results of short duration strength tests are thus not very useful for determining creep susceptibility and the type of creep mechanism.

Creep and thus squeezing can occur without volume change. In cases of dilatant behaviour, squeezing will be associated with volume increase. It is also possible that pore or cleft water dissipation occurs with squeezing; in such circumstances consolidation and volume decrease will be associated with squeezing.

- **Definition adopted in Japan (Aydan et al. 1993)**

In Japan, when tunnels exhibit large deformations during excavation, the rock is generally termed as “expansive”. Therefore, in general squeezing is regarded as a large inward closure of tunnels and no distinction is made on the nature of the motion. Phenomenologically, the squeezing type of closure may involve three possible forms of failure of the surrounding medium:

a) complete shear failure

b) buckling failure
c) shearing and sliding failure.

It is also noted that the squeezing phenomenon may be treated as having an elasto-visco-plastic behaviour and it can only occur when the rock is yielded by the redistributed state of stress following the excavation of the tunnel. It is a physical process and involves the irrecoverable dilatant behaviour of the rock. On the other hand, the swelling phenomenon is a chemical process involved with the exchange of ions between some minerals and water.

Acknowledgments

The present study has been carried out with the financial support of the Minister of the University and Scientific Research within the National Project "Tunnelling in difficult conditions", coordinated by Prof G. Barla in the Structural and Geotechnical Engineering Department of Politecnico di Torino (project n. 9708328160/1998).

CONTENTS

ABSTRACT....1

1. INTRODUCTION....2

2. IDENTIFICATION AND QUANTIFICATION OF SQUEEZING CONDITIONS....4
   - 2.1 Empirical approaches....5
   - 2.2 Semi-empirical approaches....7

3. EXCAVATION AND SUPPORT METHODS....17
   - 3.1 Brief historical retrospective....17
   - 3.2 Conventional methods....20
   - 3.3 Mechanised excavation....32

4. ANALYSIS OF ROCK MASS RESPONSE....36
   - 4.1 Closed form solutions....36
     - 4.1.1 Elasto-plastic solutions....36
     - 4.1.2 Time dependent response....41

5. ROCK-SUPPORT INTERACTION ANALYSIS....45
   - 5.1 Rock mass response....45
   - 5.2 Support response....47
   - 5.3 Numerical analyses....49
     - 5.3.1 Continuum approach....50
     - 5.3.2 Discontinuum approach....60
     - 5.3.3 Influence of 3D conditions....62

6. OBSERVATION AND MONITORING DURING EXCAVATION 68
6.1 Concepts 69
6.2 Summary of instrumentation 70
6.3 Observation and monitoring of a test tunnel 72
6.4 Convergence measurements interpretation 72
6.5 Deformation ahead of the tunnel face 74

7. A CASE EXAMPLE: THE PINGLIN TUNNEL (TAIWAN) 76

8. REFERENCES 87

APPENDIX 1 90